Optimum Heat Storage Design for Solar-Driven Absorption Refrigerators Integrated with Heat Exchanger Networks

Luis Fernando Lira-Barragán, José María Ponce-Ortega, and Medardo Serna-González
Chemical Engineering Dept., Universidad Michoacana de San Nicolás de Hidalgo, Morelia, Mich., 58060, México

Mahmoud M. El-Halwagi
Chemical Engineering Dept., Texas A&M University, College Station, TX, 77843

Adjunct Faculty at the Chemical and Materials Engineering Dept., King Abdulaziz University, Jeddah, 21589, Saudi Arabia

DOI 10.1002/aic.14308
Published online December 31, 2013 in Wiley Online Library (wileyonlinelibrary.com)

A methodology is presented for optimizing hybrid renewable energy-fossil fuel systems with short-term heat storage. The considered system is an absorption-refrigeration (AR) cycle integrated with a heat exchanger network (HEN) requiring cooling below ambient temperature. The AR cycle can be driven by multiple energy sources including excess energy from hot process streams, renewable energy sources (solar and biofuels), and fossil fuels. A two-step approach based on mixed integer nonlinear programming methods is used for the optimization. First, the problem of optimal energy integration in the hybrid energy system without heat storage is solved on a monthly basis by minimizing simultaneously the total annual cost and the overall greenhouse gas emissions. In the second step, the multi-tank thermal energy storage (TES) design problem is solved. The design involves the identification of the optimal number of storage tanks, their sizes, configuration and operation policies. The TES optimization is carried out on an hourly basis while incorporating the design targets determined by the first step. © 2013 American Institute of Chemical Engineers *AIChE J*, 60: 909–930, 2014
Keywords: heat integration, renewable energy, solar energy storage, multitank liquid water TES, heat exchanger network, absorption refrigerator, sustainable systems

Introduction

Nowadays one of the most important problems around the world is the proper use of energy because of the current depletion of nonrenewable fuels as well as the environmental issues generated when fossil fuels are used. Consequently, there is a need to replace fossil fuels with cleaner forms of energy (i.e., biofuels, solar energy, wind energy, etc.) but, at the same time, it is required to obtain economic benefits. This situation has promoted that a growing number of governments around the world have encouraged the use of clean energies through tax credits. In this sense, the chemical and petrochemical industry is now interested in using cleaner forms of energy because this is one of the most important energy consumers, which typically is obtained from fossil fuels with the aforementioned problems that require to be properly addressed.

Waste heat from hot process streams in industrial plants is removed by using different types of cooling systems. Above ambient temperature, the recirculating cooling water system is the most common method to remove the process waste heat. Several methodologies have been reported in the literature for obtaining the optimal design of these heat rejection systems (i.e., Kim and Smith[1] designed a cooling system considering all the components and the interactions between cooling water networks and the tower performance; Picón-Núñez et al.[2] introduced a methodology for designing coolers including piping costs, exchanger costs and pumping costs; Costinovis et al.[3] presented an approach for the systematic performance analysis of a cooling water system; Ponce-Ortega et al.[4] proposed an optimization for the simultaneous synthesis and detailed design of recirculating cooling water systems; Ponce-Ortega et al.[5] incorporated a disjunctive programming formulation for the optimal design of cooling water systems; Ponce-Ortega et al.[6] reported a MINLP model for synthesizing cooling networks; and Rubio-Castro et al.[7] addressed a systematic approach for the synthesis of recirculating cooling water systems involving detailed design of cooling towers, and Rubio-Castro et al.[8] applied this approach for reducing the temperatures of hot aqueous effluent streams). On the other hand, vapor-compression refrigeration systems are commonly used to remove heat from process streams at subambient temperatures. However, these refrigeration systems involve high operating costs and very expensive compressors. Absorption refrigeration (AR) cycles are an attractive alternative to mechanical refrigeration technologies to provide the necessary cooling over moderate low temperature levels at

Correspondence concerning this article should be addressed to J. M. Ponce-Ortega at jmponce@umich.mx.

reduced overall energy consumption (see Smith[9] and El-Halwagi[10]), due to they are driven by a heat source instead of electricity. High temperature heat from fossil fuels is commonly used as a heat source to run the stripper or generator of AR cycles (e.g., Ziegler and Riesch[11] and Herold et al.[12]); nevertheless, when fossil fuels are used there are significant amounts of greenhouse gas emissions (*GHGE*) released to the environment. To reduce the anthropogenic *GHGE* and the harmful climate change effects caused by them, several governments around the world have implemented incentive policies, such as carbon tax credits and subsidies, for stimulating the investment in clean and renewable energy related technologies to increase their deployment. In this context, Chavez-Islas et al.[13–15] proposed an approach for designing ammonia-water AR systems, while Florides et al.[16,17] modeled an absorption solar cooling system, Assilzadeh et al.[18] introduced a methodology for a solar cooling system using evacuated tube solar collectors and LiBr absorption unit, Lecuona et al.[19] determined the optimal hot water temperature that maximizes the efficiency of a chiller, Fathi et al.[20] studied the effect of the variables that affect the coefficient of performance (*COP*) of absorption refrigerators and Wu et al.[21] presented optimization formulations for designing AR systems. Additionally, mathematical programming approaches have been proposed to design energy systems (i.e., Savola and Fogelholm et al.[22] presented a MINLP model for increasing the power production in small scale; Tveit et al.[23] proposed a MINLP model for analyzing new investments and operation of CHP plants and Hamed et al.[24] carried out the optimization of an absorption refrigerator in dynamic mode). However, all previously mentioned approaches were developed to optimize stand-alone AR cycles without considering their heat integration with processes (i.e., hot and cold process streams).

Recently, some methodologies have addressed the optimization of AR cycles considering simultaneously economic and environmental issues. In this regard, Gebreslassie et al.[25] designed absorption refrigeration systems including environmental aspects, then Gebreslassie et al.[26] incorporated uncertainties to the model and Gebreslassie et al.[27] developed a systematic tool for solving this problem, while Ponce-Ortega et al.[28] presented a methodology for the energy integration of systems requiring refrigeration; however, in these methodologies the AR cycles also have been optimized without considering the options for heat transfer from hot process streams to the cycle generator. Consequently, the optimal integration of AR cycles with industrial processes (i.e., heat exchanger networks) is an important task, since it can yield simultaneously economic (because of the reduction of external heat sources) and environmental (because of the reduction in the associated GHGE) benefits. As pointed out by Lira-Barragán et al.,[29] efficient strategies have to be developed to incorporate heat exchanger network considerations at the design level of these integrated systems. Several methodologies have been reported in literature for synthesizing HEN including the state of the art,[30–34] which use different solution strategies including heuristic approaches (i.e., Linnhoff[35] presented a method for the design of HEN; while Linnhoff and Ahmad[36] proposed a simple methodology for the design of HEN accounting for the energy; Shenoy[37] carried out the optimization for the synthesis of HEN; Castier[38] addressed a nongraphic procedure for utility targeting in heat exchanger networks), mathematical programming approaches (i.e., Yee and Grossmann[39] developed an efficient superstructure for HEN; López-Maldonado et al.[40] presented a model formulation for synthesis of HEN minimizing the cots and environmental impact; Ponce-Ortega et al.[41] introduced a MINLP problem for the synthesis of HEN using multiple utilities) and stochastic approaches (for example Lewin[42] developed a methodology for the synthesis of HEN based on genetic algorithms; Lewin et al.[43] presented an approach for the synthesis of HEN maximizing the energy recovery; Yu et al.[44] proposed a formulation for solving a large-scale system energy integration; Ravagnani et al.[45] addressed a strategy for synthesis and optimization of HEN using genetic algorithms; Allen et al.[46] developed a procedure for the design of the components of HEN using pinch analysis and genetic algorithms; Lin and Miller[47] presented an optimization approach for synthesis of HEN through tabu search; Silva et al.[48] proposed an optimization model for HEN based on particle swarm optimization; Athier et al.[49] addressed the synthesis of HEN using simulated annealing; Dolan et al.[50] designed a methodology for the optimization of HEN through simulated annealing technique based on the Monte Carlo method; Lotfi and Boozarjomehry[51] presented the synthesis of HEN using modular simulators and genetic algorithms, and Ponce-Ortega et al.[52] proposed a methodology for the optimal synthesis of multipass HEN).

The synthesis problem of an AR cycle integrated with a HEN using multiple energy sources (solar energy, biofuels, and fossil fuels) was formulated by Lira-Barragán et al.[29] as a mixed integer nonlinear programming problem, which accounts simultaneously for economic, environmental and social criteria as objective functions. Also, it includes the optimal selection of clean forms of energy (solar and biofuels) to run the cycle generator or striper. This approach showed that the use of renewable energy sources (solar energy and biofuels) in conjunction with hot process streams as heat sources reduces significantly the burning of fossil fuels and, thus, reduces the emission of pollutants and *GHGE* in refrigeration systems integrated with chemical processes. This approach also yields economic benefits due to the tax credits associated with the use of renewable energy sources. The authors use a monthly average solar radiation to determine the optimal solar integration with the process and other energy sources (fossil fuels and biofuels) required to meet the daily energy demands of the overall system, without considering thermal storage of solar energy. However, this is not the case for actual solar-driven absorption refrigerators integrated with industrial processes (see Figure 1), since the solar radiation constantly varies and is only available for a portion of each 24-h day (i.e., 8 to 12 h/day). As a result, both the energy collected and the temperature of the solar collector vary significantly during the day and season, which in turn causes an hourly variation in cooling capacity of AR cycles. Therefore, in addition to monthly average solar radiation, the variability of the incidence solar irradiance throughout the day must be taken into account along with thermal energy storage of solar energy to keep the cooling system capacity steady.

In light of the aforementioned issues, this article presents a systematic mathematical framework for incorporating short-term heat storage in hybrid renewable energy-fossil fuel systems consisting of an AR cycle integrated with a HEN. This is an extension of the optimization model proposed by Lira-Barragán et al.[29] where no heat storage aspects were addressed. A key feature of this work is the use of a multitank thermal energy (TES) storage subsystem that

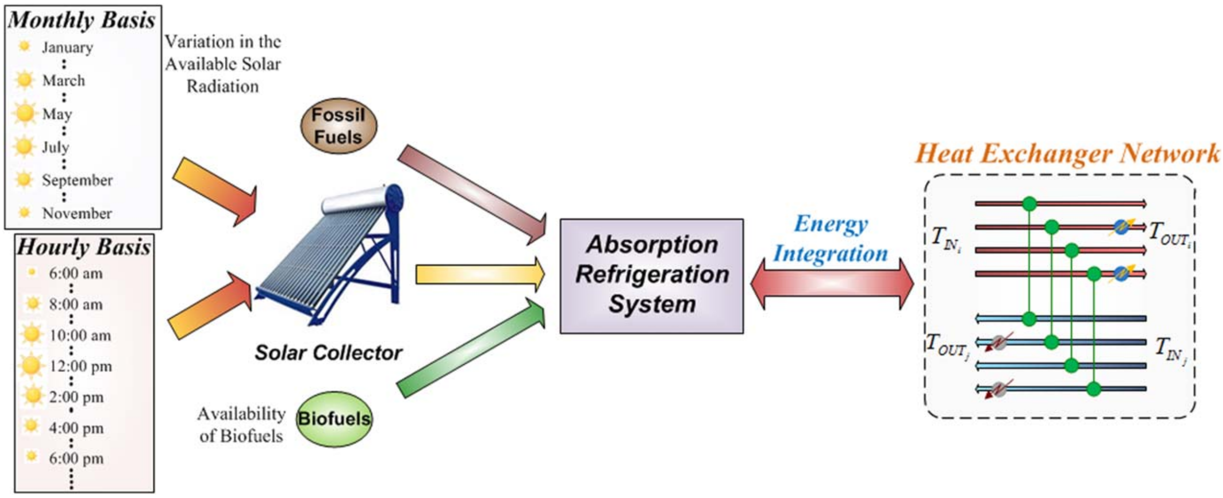

Figure 1. Schematic representation of the addressed problem considering the temporally variable availability of solar radiation in the synthesis of hybrid energy systems.

[Color figure can be viewed in the online issue, which is available at wileyonlinelibrary.com.]

we propose to solve the hourly variability problem of solar energy and, hence, enhance the reliability and overall performance of solar-driven absorption refrigerators that must operate 24 h. It uses liquid water as both the heat transfer fluid and the heat storage medium. A two-step approach based on mixed integer nonlinear programming methods is used to solve the overall problem. The first step in this methodology optimizes the configuration and design of the HEN coupled with the AR cycle without heat storage on a monthly basis. This solution gives the process heating and cooling requirements, as well as the heat load of the AR cycle. In addition, in the first step the type of the solar collector and the optimum size (i.e., area) of the solar collector field are determined to meet the AR generator heating demand according to the monthly average solar radiation data. In the second step, the design and operation of the multitank energy storage subsystem for a selected design determined in the first step is accomplished taking into account hourly variations in solar radiation to satisfy the process and AR cycle heat loads throughout the day. This is a complex problem due to the considerable amount of variables and decisions involved such as the period of the short-term storage, the size of the storage system (e.g., the number and size of storage tanks), the operating conditions (temperature difference over which the storage media is used and liquid water mass flow rate in the solar collectors) and the operational strategy (catching and dispatching of hot water), as well as a number of constraints that must be satisfied. To tackle this problem, a multiperiod mixed integer nonlinear model is developed. This formulation provides the optimum TES subsystem design and its optimum operation strategy for each period of operation. The application of the two-step proposed approach is illustrated with two case studies.

Problem Statement

The problem addressed in the article is stated as follows. Given are:

- A set of hot process streams which have to be cooled (some of them require cooling below ambient temperature), and a set of cold process streams which have to be heated.
- A set of solar collectors available to catch the solar energy.
- A set of thermal storage tanks (hot tanks) which are needed for storing solar energy as heat to meet the absorption-refrigeration heat duty when sunlight is not available (i.e., during nights and cloudy days).
- The economic data and operational constraints for the low temperature storage tank (cold tank), where the cold water coming from the AR cycle is collected until it is pumped back to the solar collector field.
- A set of available biofuels B, a set of available fossil fuels F, and a backup boiler that can make use of biofuels and fossil fuels to meet the heating demand of the AR generator when the solar resource is not available or is insufficient.
- Cooling water to cool hot process streams and low pressure steam to heat cold process streams.

Then, the problem consists in determining the optimal design of the HEN coupled with the AR cycle including the optimum size of the solar collector field, as well as the optimal design and operation of the heat storage subsystem taking into account monthly and hourly variations in solar radiation, and accounting for the tradeoffs between the economic, environmental and social objectives.

Solution Strategy

To solve the aforementioned problem, the solution strategy shown in Figure 2 is implemented. This strategy consists of the following steps:

- **Input data.** The following data are needed to optimizing the considered hybrid energy system: the stream data of the process streams; the characteristics of the absorption refrigeration system; the type of available solar collectors, including their efficiency to collect the useful solar energy for the specific location where the solar collector must be installed; monthly average values and hourly values of solar radiation, at the system location; the fossil fuels and biofuels available to be used, as well as their unitary costs, the unitary emissions (which can be obtained using software like GREET or BESS[53,54]) and the number of jobs[55] that can be generated by each fuel; the type of available storage tanks and the maximum available volume for each one; and finally the data for utilities (auxiliary heating and cooling) and the minimum temperature difference.

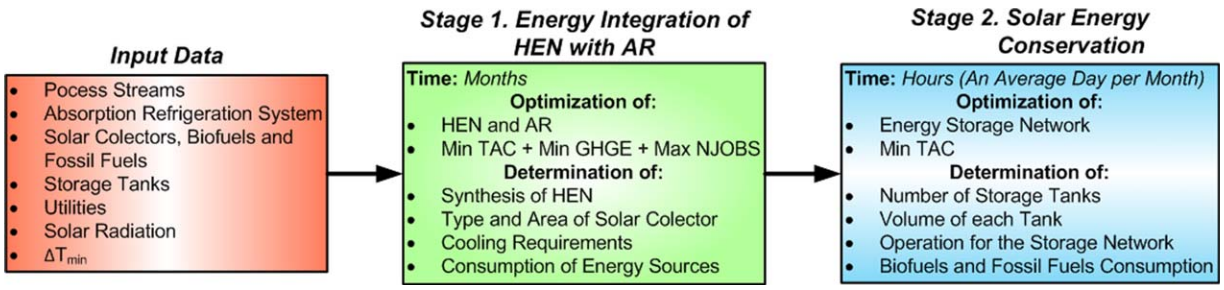

Figure 2. Proposed solution strategy.

[Color figure can be viewed in the online issue, which is available at wileyonlinelibrary.com.]

• **Step 1**. In this step, the multiobjective optimization MINLP formulation by Lira-Barragán et al.[29] is used to obtain the Pareto optimal solution for each month of the hybrid energy system under study without heat storage of solar energy. The problem consists in minimizing simultaneously the total annual cost (*tac*) and the overall *GHGE* (*nghge*) accounting for the overall number of jobs (*njobs*) created by the project. Figure 3 shows a representation of the hybrid energy system superstructure. First, in the superstructure the hot process streams can transfer heat to the stripper located inside the absorption refrigeration cycle (to reduce the consumption of external energy sources), which requires a minimum temperature of 80°C; after it there is allowed the heat transfer between process streams into a set of inner stages, where the number of stages is determined as the maximum of hot or cold process streams. The next stage represents a first cooling stage for hot process streams using cooling water (CW) (i.e., available at 30°C). Finally, for the hot process streams that require cooling below room temperature, a set of coolers is placed at the cold-end (AR2) of the system to reach the target temperatures. For the cold process streams, the first stage consists in the matching between hot and cold process streams to enhance heat recovery in the inner stages of the superstructure; then, at the hot-end of the system, the cold process streams that still have not reached their target temperatures can be processed through a set of heaters that use low pressure steam (LPS) as hot utility. It should be noticed that this configuration was determined based on the temperature levels for the streams to provide the optimal solution.

On the other hand, in this work each Pareto optimal solution provides the following information: the configuration

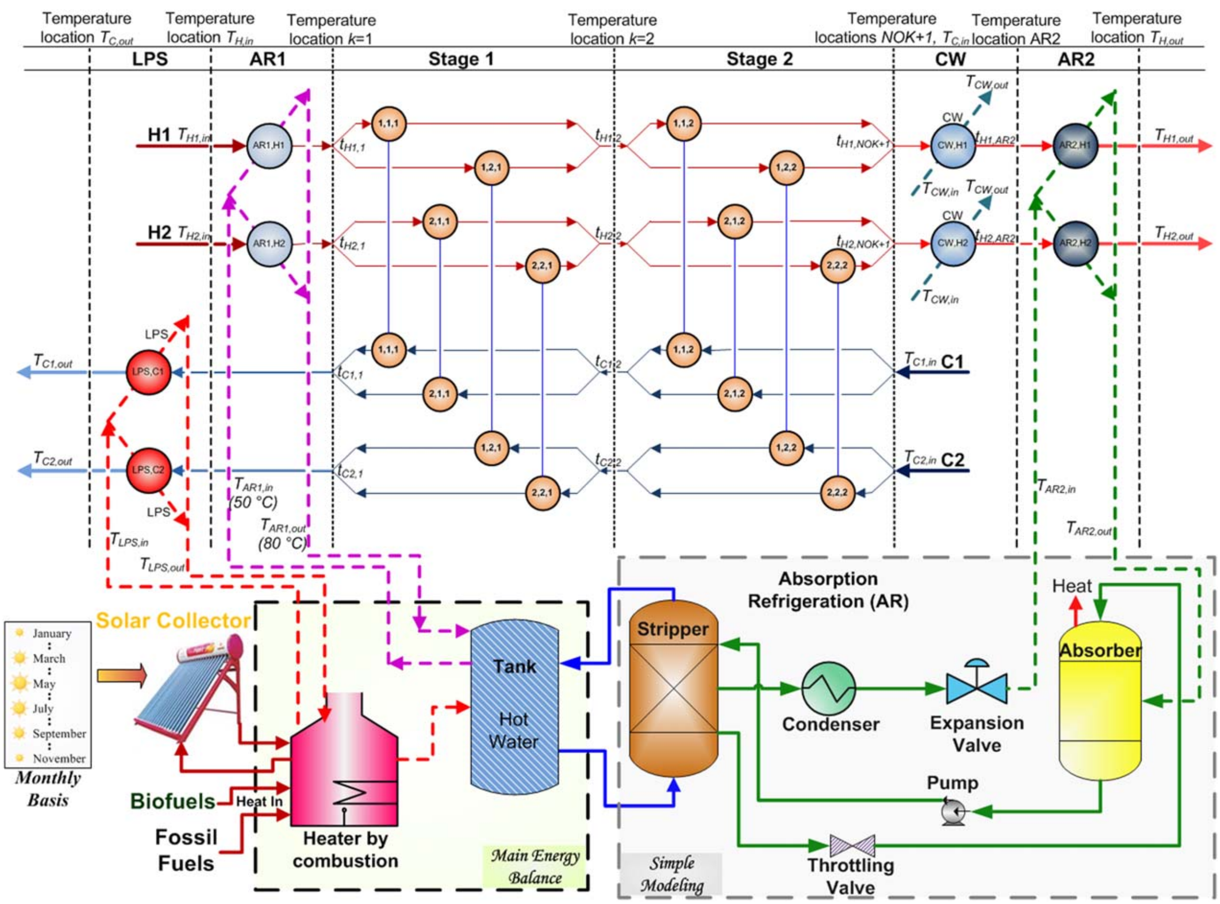

Figure 3. Superstructure of the hybrid energy system without heat storage.

[Color figure can be viewed in the online issue, which is available at wileyonlinelibrary.com.]

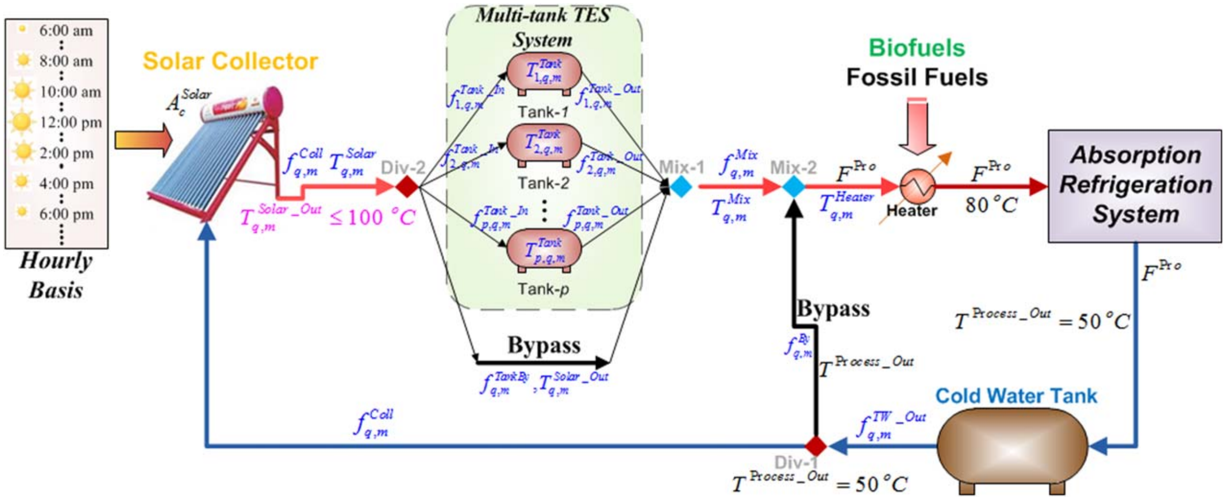

Figure 4. Superstructure for heat storage from the solar collector field.

[Color figure can be viewed in the online issue, which is available at wileyonlinelibrary.com.]

and design of the HEN (including the size and the heat transferred in each heat exchanger unit required), the type of solar collector as well as the optimal area of the solar field required to operate during the different months accounting for the variation of the available solar radiation in a given location, the cooling requirements, the solar energy demand, and the consumption of each fossil fuel and biofuel considered. Since there are no variations of operating conditions at the process, the optimal amount of excess process heat determined to drive the AR cycle and the optimal refrigeration duty of the process are taken as their steady-state values for each month. As well, the optimal requirements of external energy sources remain constant for each month. Finally, notice that this step is carried out in a monthly horizon for the supplies of the external energy sources (solar, biofuels and fossil fuels), so the hourly solar radiation variation is not considered at this level of the proposed methodology.

- **Step 2.** Once the optimum overall system is obtained without heat storage (i.e., optimum configuration and design of the HEN coupled with the AR cycle including the solar collector area), in the second step the optimum design and operation of the heat storage subsystem is determined in such a way that meets the heat load of the AR cycle during noninsolation periods. As a result, the production of the refrigeration utility in the AR cycle can be constant without fluctuations; also, the HEN can operate at nominal conditions (i.e., steady-state operation) regardless of whether the sun is shining at full or partial strength, or whether it is cloudy or nighttime.

Figure 4 shows the superstructure for the thermal energy storage proposed, in which liquid water is used as both the heat-transfer fluid and the storage medium. Hence, liquid water moves heat from the solar collector field to the TES subsystem and the AR cycle. In the solar field the cold water can be heated up to 100°C (the boiling point of the water at 1 bar) with concentrated solar energy. The solar field provides an excess of heat over and above the heat demanded by the AR system during the solar period. This excess heat is stored to be used in periods when heat from the solar field is not enough to drive the AR cycle. The TES subsystem consists of a set of hot storage tanks connected in parallel and a cold storage tank. Depending on the optimal solution, each of the hot tanks may exist or not. The advantage of this multitank configuration for the TES subsystem is that hot and cold water are stored separately.

As can be seen in Figure 4, the total hot water stream leaving the solar collector field is divided by splitter Div-2 into smaller streams that enter each individual hot storage tank and a bypass stream that is directed to the mixer Mix-1 at the outlet of the set of hot storage tanks. This mixer generates the inlet stream to the generator of the AR cycle which consists of a total hot water stream originated from the outlets streams of all the hot storage tanks, the bypass stream of the hot tanks, and a cold water stream originated from the cold storage tank. Each of these streams may or may not be activated in the optimal solution. Only when the hot water produced by solar collectors or leaving hot storage tanks is warmer than the required temperature (80°C) to drive the AR cycle, the cold water stream coming from the cold storage tank is used to adjust the temperature of the outlet stream from the mixer. Contrarily, this stream must pass through an auxiliary heater that uses backup fuels (biofuels and fossil fuels) to warm the water when its temperature is lower than the desired set temperature. Thus, backup resources avoids that the hybrid energy system performs at part-load conditions when solar energy is not available and heat from the hot storage tanks is not enough to drive the AR cycle.

On the other hand, the cooled water at 50°C from the AR cycle flows to the low-temperature storage tank, the outlet of which is divided by splitter Div-1 into a total cold water stream that is returned to the solar collector field and a second stream that feeds Mix-2. When there is no or not enough solar radiation, the solar collector field is bypassed since it does not make sense to pump water to the collectors when they cannot work. In this case, the cold water is sent directly to the auxiliary heater and/or remains at constant temperature (50°C) in the low-temperature storage tank. So, this tank allows controlling the flow rates of the cold water streams feed to the solar collector field and Mix-2 to meet the desired set temperature of the AR cycle throughout the day. Therefore, the proposed superstructure allows the optimal management of cold water before it returns to the solar collector field, thus providing a better energy management strategy for the integrated TES subsystem. It should be noted that the proposed heat storage along with the auxiliary heater allows the hybrid energy system to operate always at steady state (nominal conditions) like a conventional system based only on fossil-fuels due to the production of heating utility can be constant without intermittence.

For the analysis presented here, the following operation strategy of the storage subsystem is applied: the AR cycle always has priority in operation, so AR generator comes before storage charging. Only if the thermal energy collected by the solar field exceeds the design value of the AR generator heat load, the surplus energy is fed into the thermal storage tanks. On the other hand, if the thermal energy collected by the solar field is lower than the design value, additional energy will be taken from the storage. By this means, the AR cycle can be operated at full load with high efficiency even under low radiations conditions. Discharging of the storage and operation of the AR cycle continues after sunset until the storage is discharged again. The storage is used in a way that the AR cycle can be operated at full load as much as possible without burning fossil fuel in the auxiliary heater. Thus, the operation strategy adopted for the hybrid energy system with heat storage considered is the scheduled mode, instead of the solar dispatching mode.

In the second step, the simultaneous design and scheduling problems for the TES subsystem are formulated as a multiperiod mixed integer nonlinear problem. We take advantage of the knowledge of scheduling optimization procedures that have been published recently. The reviews by Mendez et al.[56], Floudas and Lin[57], Kallrath[58] and Barbosa-Povoa[59] highlighted the importance of scheduling optimization methods in the process industry, whereas other authors have successfully applied such techniques to solve various manufacturing problems (for example, Mouret et al.[60] introduced a methodology to solve large-scale MINLP problems for the oil refining industry considering planning and scheduling, then Mouret et al.[61] incorporated priority slots; Sharda and Vazquez et al.[62] presented a discrete event simulation decision support system to evaluate tank farm operations; Terrazas-Moreno et al.[63] proposed a MILP formulation for the tank farm operation problem; Gutiérrez-Limón et al.[64] developed a multiobjective formulation dealing with simultaneous scheduling and control issues in processing systems; Erdirik-Dogan and Grossmann[65] presented a multi-period MILP model for the planning and scheduling of single-stage plants; Barbosa-Povoa and Macchietto[66] proposed a formulation for the optimal selection of equipment units and the network of connections for multipurpose batch plants; Lin and Floudas[67] synthesized a multipurpose batch plant considering scheduling issues; Castro et al.[68] presented a general mathematical formulation for the simultaneous design and scheduling of multipurpose plants). However, there have not been yet works for optimizing simultaneously both the design and operation strategy of short-term heat storage in solar-driven absorption refrigerators integrated with heat exchanger networks for the optimal solar energy conservation considering an average day per month and a discretization for time of 1 h accounting for 24 slots.

The proposed multiperiod MINLP formulation consists of minimizing the total annual cost (TAC) of the TES subsystem, which is composed by the capital costs for the storage tanks, as well as the cost of backup fuels (fossil fuels and biofuels). For the optimization of the TES subsystem, an hourly calculation is performed using hourly solar radiation values. The optimal solution of this problem provides the number, distribution and capacity of hot storage tanks required, in addition to the operation for the storage subsystem including the catching and dispatching of the storage tanks as well as the variation of water flow rates over a short time horizon (e.g., days).

Next, the mathematical model developed to solve the problem under study is presented in detail.

Model Formulation

The first part of the proposed solution strategy is to collect the required data that describe the system (according to Figure 2). Once the needed information is available, then it is applied the following optimization stages.

Model Formulation for First Step: HEN Integrated with an AR Cycle

The mathematical programming model used to carry out the energy integration of heat exchanger networks with solar-driven absorption refrigerators is based on the superstructure presented in Figure 3. The formulation is composed by the HEN model and the AR model (including the reformulation of a disjunctive model to select the type of the solar collector). The relationships associated with this model are presented as follows.

Heat exchanger network

The constraints that applied to the HEN are the following.

Total Energy Balances for the Process Streams. The heat load of each hot process stream i is equal to the sum of heat loads that it exchanges with the AR cycle q_i^{ar1} (only for hot process streams above 80°C), with the cold process streams $q_{i,j,k}$, with the cooling water q_i^{cw} and/or with the refrigeration subsystem at low-temperature q_i^{ar2};

$$(T_i^{IN}-T_i^{OUT})FCp_i=q_i^{ar1}+\sum_{k\in ST}\sum_{j\in CPS}q_{i,j,k}+q_i^{cw}+q_i^{ar2}, \qquad \forall i\in HPS \tag{1.1}$$

The heat required for any cold process stream j can be expressed as the sum of the heat loads that it absorbs from hot process streams $q_{i,j,k}$ and/or from low-pressure steam q_j^{LPS}

$$(T_j^{OUT}-T_j^{IN})FCp_j=\sum_{k\in ST}\sum_{i\in HPS}q_{i,j,k}+q_j^{LPS}, \qquad \forall j\in CPS \tag{1.2}$$

Energy Balances for Matches at each Inner Stage of the Superstructure. Equations 1.3 and 1.4 below describe the energy balances for each match between hot stream i and cold stream j at the inner stage k of the superstructure,

$$(t_{i,k}-t_{i,k+1})FCp_i=\sum_{j\in CPS}q_{i,j,k}, \forall i\in HPS, k\in ST \tag{1.3}$$

$$(t_{j,k}-t_{j,k+1})FCp_j=\sum_{i\in HPS}q_{i,j,k}, \forall j\in CPS, k\in ST \tag{1.4}$$

Energy Balances for Matches between Hot Process Streams and Absorption Refrigeration Subsystem. Only hot process streams with inlet temperatures above 80°C can transfer their heat excess to the absorption refrigeration cycle at the hottest side of the superstructure

$$(T_i^{IN} - t_{i,1})FCp_i = q_i^{ar1}, \forall i \in HPS \quad (1.5)$$

Similarly, the refrigeration for the hot process streams is determined as follows

$$(t_i^{ar2} - T_i^{OUT})FCp_i = q_i^{ar2}, \forall i \in HPS \quad (1.6)$$

Balances for Steam and Cooling Water Utilities. The heat removed from hot process streams using cooling water is determined as follows

$$(t_{i,NOK+1} - t_i^{ar2})FCp_i = q_i^{cw}, \forall i \in HPS \quad (1.7)$$

while the hot utility needed to satisfy the heating requirement of each cold process stream is determined as follows

$$(T_{OUT_j} - t_{j,1})FCp_j = q_j^{LPS}, \forall j \in HPS \quad (1.8)$$

Temperatures Assignment for the Extreme Borders of the Superstructure. In the proposed configuration, the inlet temperatures of the cold process streams define the temperatures at the last border ($k = NOK + 1$) of the superstructure

$$T_j^{IN} = t_{j,NOK+1}, \forall j \in CPS \quad (1.9)$$

Feasibility Constraints of Temperature. The following set of constraints establishes that there must be a monotonic decrease of temperature at each successive stage from the lefthand side to the righthand side of the superstructure

$$T_i^{IN} \geq t_{i,1}, \forall i \in HPS \quad (1.10)$$

$$t_{i,k} \geq t_{i,k+1}, \forall i \in HPS, k \in ST \quad (1.11)$$

$$t_{i,NOK+1} \geq t_i^{ar2}, \forall i \in HPS \quad (1.12)$$

$$t_i^{ar2} \geq T_i^{OUT}, \forall i \in HPS \quad (1.13)$$

$$T_j^{OUT} \geq t_{j,1}, \forall j \in CPS \quad (1.14)$$

$$t_{j,k} \geq t_{j,k+1}, \forall j \in CPS, k \in ST \quad (1.15)$$

Existence of the Heat Exchanger Units. The existence of heat-transfer units between hot and cold process streams in any stage of the superstructure is determined by the following constraint

$$q_{i,j,k} - Q_{i,j}^{\max} z_{i,j,k} \leq 0, \forall i \in HPS, j \in CPS, k \in ST \quad (1.16)$$

Similar relationships apply for the hot process streams that transfer heat to the absorption refrigeration cycle ($q_i^{ar1} - Q_i^{\max} z_i^{ar1} \leq 0, \forall i \in HPS$), for the matches between the hot process streams and cooling water ($q_i^{cw} - Q_i^{\max} z_i^{cw} \leq 0, \forall i \in HPS$), between hot process streams and the absorption refrigeration at the cold side ($q_i^{cw} - Q_i^{\max} z_i^{cw} \leq 0, \forall i \in HPS$), and for the match between cold process streams with heating utility ($q_j^{LPS} - Q_j^{\max} z_j^{LPS} \leq 0, \forall j \in CPS$). In previous relationships, $Q^{\max}$ is an upper bound for the heat exchanged in each unit.

Feasibility Constraints of the Temperature Differences. To ensure thermodynamic feasibility for heat transfer, positive temperature differences are required for the different matches between hot and cold streams in the superstructure. For heat exchanger units in the inner stages, these constraints are given as follows:

$$dt_{i,j,k} \leq t_{i,k} - t_{j,k} + \Delta T_{i,j}^{\max}(1 - z_{i,j,k}), \forall i \in HPS, j \in CPS, k \in ST \quad (1.17)$$

$$dt_{i,j,k+1} \leq t_{i,k+1} - t_{j,k+1} + \Delta T_{i,j}^{\max}(1 - z_{i,j,k}), \forall i \in HPS, j \in CPS, k \in ST \quad (1.18)$$

Similar relationships are used for the other heat-transfer units. For example, for matches between hot process streams and the absorption refrigeration cycle at high-temperature levels $dt_i^{ar1-2} \leq t_{i,1} - T_{IN}^{ar1} + \Delta T_i^{ar1\max}(1 - z_i^{ar1}), \forall i \in HPS$ and $dt_i^{cw1} \leq t_{i,NOK+1} - T_{OUT}^{cw} + \Delta T_i^{cw\max}(1 - z_i^{cw}), \forall i \in HPS$, for cooler using cooling water $dt_i^{cw2} \leq t_i^{ar2} - T_{IN}^{cw} + \Delta T_i^{cw\max}(1 - z_i^{cw})$, $\forall i \in HPS$, and $dt_i^{ar2-1} \leq t_i^{ar2} - T_{OUT}^{ar2} + \Delta T_i^{ar2\max}(1 - z_i^{ar2}), \forall i \in HPS$, and for heaters using low-pressure steam $dt_j^{LPS-2} \leq T_{OUT}^{LPS} - t_{j,1} + \Delta T_j^{LPS\max}(1 - z_j^{LPS}), \forall j \in CPS$. In previous relationships is used as upper limit.

Finally, the following constrains ensure the fulfillment of the minimum temperature difference in all heat-transfer units

$$\Delta T_{\min} \leq dt_{i,j,k}, \forall i \in HPS, j \in CPS, k \in ST \quad (1.19)$$

However, similar relationships apply for absorption refrigeration cycle and hot process streams at the hot side $\Delta T_{\min} \leq dt_i^{ar1-2}, \forall i \in HPS$, for the matches between hot process streams and cooling water $\Delta T_{\min} \leq dt_i^{cw1}, \forall i \in HPS$, between hot process streams and the absorption refrigeration cycle at the cold side $\Delta T_{\min} \leq dt_i^{ar2-1}$, $\forall i \in HPS$, and for the match between cold process streams and low-pressure steam $\Delta T_{\min} \leq dt_j^{LPS-2}, \forall j \in CPS$. $\Delta T_{\min}$ is the minimum temperature difference for any heat exchanger unit.

Absorption refrigeration cycle

Energy Balance of the Absorption Refrigeration Cycle. The heating requirements of the cold process streams that are supplied by the low-pressure steam $\frac{\sum_{j \in CPS} q_j^{LPS}}{COP^{LPS}}$ plus the energy required to run the refrigeration system $\frac{\sum_{i \in HPS} q_i^{ar2}}{COP^{ar2}}$ is equal to the energy provided to the absorption refrigeration system by the hot process streams at high temperature plus the energy obtained from fossil fuels q_i^{ar1}, biofuels $q_{b,m}^{Biofuel}$ and the solar collector q_m^{Solar}

$$\frac{\sum_{j \in CPS} q_j^{LPS}}{COP^{LPS}} + \frac{\sum_{i \in HPS} q_i^{ar2}}{COP^{ar2}} = \sum_{i \in HPS} q_i^{ar1} + \sum_{f \in F} q_{f,m}^{Fossil} + \sum_{b \in B} q_{b,m}^{Biofuel} + q_m^{Solar}, \forall m \in M \quad (1.20)$$

Notice in the previous equation that this is stated for each month (m) of the year to properly account for the seasonal variation of the available solar radiation as well as the availability of the biofuels. In this relationship COP^{LPS} and COP^{ar2} are the coefficient of performance for the steam and absorption refrigeration subsystems, respectively (see Tora and El-Halwagi[69]).

Model of the Solar Collectors. The optimization model can select the type of collector to be used according to the following disjunction

$$\bigvee_{s\in S}\left[\begin{array}{c} Y^{Solar} \\ c^{Tank}=FC^{Tank}+VC^{Tank}\left(v^{Tank}\right) \\ \left[\begin{array}{c} Z_s^{Solar} \\ q_m^{Solar} \le Q_{s,m}^{Useful\_Solar} a_c^{Solar} \dfrac{1}{D_m^{sm}}, \forall m \in M \\ c_{op}^{Solar}=Cu_s^{Solar} \sum_{m\in M}\left(q_m^{Solar} D_m^{sm}\right) \\ \left[\begin{array}{c} W_{s,1}^{Solar} \\ A_{s,1} \le a_c^{Solar} \le A_{s,2} \\ c_{cap}^{Solar}=FC_{s,1}^{Solar}+VC_{s,1}^{Solar}\left(a_c^{Solar}\right) \end{array}\right] \vee \left[\begin{array}{c} W_{s,2}^{Solar} \\ A_{s,2} \le a_c^{Solar} \le A_{s,3} \\ c_{cap}^{Solar}=FC_{s,2}^{Solar}+VC_{s,2}^{Solar}\left(a_c^{Solar}\right) \end{array}\right] \vee \cdots \vee \left[\begin{array}{c} W_{s,G}^{Solar} \\ A_{s,G} \le a_c^{Solar} \le A_{s,G+1} \\ c_{cap}^{Solar}=FC_{s,G}^{Solar}+VC_{s,G}^{Solar}\left(a_c^{Solar}\right) \end{array}\right] \end{array}\right] \end{array}\right] \vee \left[\begin{array}{c} \neg Y^{Solar} \\ c^{Tank}=0 \\ q_m^{Solar}=0 \\ a_c^{solar}=0 \\ c_{op}^{Solar}=0 \\ c_{cap}^{Solar}=0 \end{array}\right]$$

In this disjunction, Y^{Solar} is a Boolean variable associated with the existence of the solar collector; thus, if Y^{Solar} is true, a solar collector is required; otherwise, when the Boolean variable is false, the solar collector is not required and all the variables included in the disjunction are set to zero. Additionally, if the solar collector is required, then one type of solar collector must be selected. In this regard, Z_s^{Solar} is the Boolean variable associated with the type of the solar collector. The model is suitable to consider several solar collectors with different costs and different efficiencies to capture the solar radiation per unit of area; consequently, using the efficiencies and the solar radiation data is possible to obtain the value of $Q_{s,t}^{Useful\_Solar}$ for each collector (notice that once the optimization process has been carried out, the optimal size a_c^{Solar} for the solar collector must be determined; therefore, the total solar energy q_m^{Solar} per month can be calculated). The cost function of solar collectors is nonlinear and it includes a fixed charge term (FC_s^{Solar}) and a variable charge term (VC_s^{Solar}). Thus, to avoid the nonlinear terms, the disjunctive model also considers the linearization of the cost function through sectioning it on several linear segments. The convex hull technique is used to reformulate previous disjunction. The reformulation converts the Boolean variables into a set of binary variables and yields the next algebraic relationships. First, only one type of solar collector can be selected

$$y^{Solar}=\sum_{s\in S} z_s^{Solar} \tag{1.21}$$

Then, the continuous variables are disaggregated

$$z_s^{Solar}=\sum_{g\in G} \widehat{w}_{s,g}^{Solar}, \forall s \in S \tag{1.22}$$

$$q_m^{Solar}=\sum_{s\in S} \widehat{q}_{m,s}^{Solar}, \forall m \in M \tag{1.23}$$

$$a_c^{Solar}=\sum_{s\in S} \widehat{a}_{c_s}^{Solar} \tag{1.24}$$

$$\widehat{a}_{c_s}^{Solar}=\sum_{g\in G} \widehat{a}_{c_{s,g}}^{dis}, \forall s \in S \tag{1.25}$$

$$c_{op}^{Solar}=\sum_{s\in S} \widehat{c}_{op_s}^{Solar} \tag{1.26}$$

$$c_{cap}^{Solar}=\sum_{s\in S} \widehat{c}_{cap_s}^{Solar} \tag{1.27}$$

$$\widehat{c}_{cap_s}^{Solar}=\sum_{g\in G} \widehat{c}_{cap_{s,g}}^{dis}, \forall s \in S \tag{1.28}$$

The relationships are stated in terms of the disaggregated variable as follows:

$$c^{Tank}=FC^{Tank} y^{Solar}+VC^{Tank}\left(v^{Tank}\right) \tag{1.29}$$

$$\widehat{q}_{m,s}^{Solar} \le Q_{m,s}^{Useful\_Solar} \widehat{a}_{c_s}^{Solar} \frac{1}{D_m^{sm}}, \forall m \in M, s \in S \tag{1.30}$$

$$\widehat{c}_{op_s}^{Solar}=Cu_s^{Solar} \sum_{m\in M}\left(\widehat{q}_{m,s}^{Solar} D_m^{sm}\right), \forall s \in S \tag{1.31}$$

$$A_{s,g} w_{s,g}^{Solar} \le \widehat{a}_{c_{s,g}}^{dis} \le A_{s,g} w_{s,g}^{Solar}, \forall g \in G, s \in S \tag{1.32}$$

$$\widehat{c}_{cap_{s,g}}^{dis}=FC_{s,g}^{Solar} \widehat{w}_{s,g}^{Solar}+VC_{s,g}^{Solar}\left(\widehat{a}_{c_{s,g}}^{dis}\right), \forall g \in G, s \in S \tag{1.33}$$

Upper and lower bounds are required for all the disaggregated variables as follows

$$Q_{Min}^{Solar} z_s^{Solar} \le \widehat{q}_{m,s}^{Solar} \le Q_{Max}^{Solar} z_s^{Solar}, \forall m \in M, s \in S \tag{1.34}$$

$$A_{c_s}^{Solar\_Min} z_s^{Solar} \le \widehat{a}_{c_s}^{Solar} \le A_{c_s}^{Solar\_Max} z_s^{Solar}, \forall s \in S \tag{1.35}$$

$$C_{op_s}^{Min} z_s^{Solar} \le \widehat{c}_{op_s}^{Solar} \le C_{op_s}^{Max} z_s^{Solar}, \forall s \in S \tag{1.36}$$

$$C_{cap_s}^{Min} z_s^{Solar} \le \widehat{c}_{cap_s}^{Solar} \le C_{cap_s}^{Max} z_s^{Solar}, \forall s \in S \tag{1.37}$$

$$C_{cap_s}^{Min} \widehat{w}_{s,g}^{Solar} \le \widehat{c}_{cap_{s,g}}^{dis} \le C_{cap_s}^{Max} \widehat{w}_{s,g}^{Solar}, \forall s \in S, g \in G \tag{1.38}$$

Maximum Availability of the Fuels. Usually, the production of biofuels is limited during the year; in this regard, the proposed model takes into account the seasonal availability of the biofuels

$$q_{b,t}^{Biofuel} \le \frac{Heating_b^{Power} Avail_{b,t}^{Max}}{D_t}, \forall b \in B, \forall t \in T \tag{1.39}$$

where $Heating_b^{Power}$ is the heating power of biofuel *b,* and $Avail_{b,t}^{Max}$ is the maximum amount of biofuel *b* available in period *t*.

Additionally, if the availability of fossil fuels is restricted, the following constraint must be included in the model:

$$q_{f,t}^{Fossil} \le \frac{Heating_f^{Power} Avail_{f,t}^{Max}}{D_t}, \forall f \in F, \forall t \in T \tag{1.40}$$

Objective functions

In this optimization step the solutions are presented through Pareto curves, which are obtained using the epsilon-constraint methodology.[70] These Pareto curves show the economic objective function (minimization of the total annual cost) vs. the environmental objective function (minimization of the net GHGE) and the social function (the maximization of jobs generated by the project) are evaluated for all the solutions obtained. This is modeled as follows

$$OF=\left\{Min\,tac; Min\,nghge^{Overall}; Max\,jobs\right\} \tag{1.41}$$

Economic Objective Function. This objective function consists in minimizing the total annual cost, which is expressed as the sum of the heat exchanger network cost and the absorption refrigeration system cost minus the tax credits obtained by the reduction in the greenhouse gas emissions achieved for using clean energies. The heat exchanger network cost includes the capital costs for all heat-transfer units needed (in this work the Chen approximation[71] is used to calculate the log-mean temperature differences for the heat exchangers units to avoid logarithmic terms in the optimization model) and the cooling water cost. Since the proposed configuration considers the production of the hot utility (LPS), the economic function does not involve the cost of this utility.

$$\begin{aligned}
Min\,tac= & \\
+K_f & \left[\begin{aligned}
&\sum_{i\in HPS}\sum_{j\in CPS}\sum_{k\in ST} C^{exc}_{F_{i,j}} z_{i,j,k} + \sum_{i\in HPS} C^{ar1}_{F_i} z^{ar1}_i + \sum_{i\in HPS} C^{cw}_{F_i} z^{cw}_i + \sum_{i\in HPS} C^{ar2}_{F_i} z^{ar2}_i + \sum_{j\in CPS} C^{LPS}_{F_j} z^{LPS}_j \\
&+\sum_{i\in HPS}\sum_{j\in CPS}\sum_{k\in ST} C^{exc}_{i,j}\left\{\frac{q_{i,j,k}\left(\frac{1}{H_i}+\frac{1}{H_j}\right)}{\left[\left(dt_{i,j,k}\right)\left(dt_{i,j,k+1}\right)\left(\frac{dt_{i,j,k}+dt_{i,j,k+1}}{2}\right)+\delta\right]^{1/3}}\right\}^{\beta} \\
&+\sum_{i\in HPS} C^{ar1}_i\left\{\frac{q^{ar1}_i\left(\frac{1}{H_i}+\frac{1}{H_{ar1}}\right)}{\left[\left(T_{IN_i}-T^{ar1}_{OUT}\right)\left(dt^{ar1-2}_i\right)\left(\frac{\left(T_{IN_i}-T^{ar1}_{OUT}\right)+dt^{ar1-2}_j}{2}\right)+\delta\right]^{1/3}}\right\}^{\beta} \\
&+\sum_{i\in HPS} C^{cw}_i\left\{\frac{q^{cw}_i\left(\frac{1}{H_i}+\frac{1}{H_{cw}}\right)}{\left[\left(dt^{cw1}_i\right)\left(dt^{cw2}_i\right)\left(\frac{dt^{cw1}_i+dt^{cw2}_i}{2}\right)+\delta\right]^{1/3}}\right\}^{\beta} \\
&+\sum_{i\in HPS} C^{ar2}_i\left\{\frac{q^{ar2}_i\left(\frac{1}{H_i}+\frac{1}{H_{ar2}}\right)}{\left[\left(dt^{ar2-1}_i\right)\left(T_{OUT_i}-T^{ar2}_{IN}\right)\left(\frac{dt^{ar2-1}_i+\left(T_{OUT_i}-T^{ar2}_{IN}\right)}{2}\right)+\delta\right]^{1/3}}\right\}^{\beta} \\
&+\sum_{j\in CPS} C^{LPS}_j\left\{\frac{q^{LPS}_j\left(\frac{1}{H_j}+\frac{1}{H_{LPS}}\right)}{\left[\left(T^{LPS}_{IN}-T_{OUT_j}\right)\left(dt^{LPS-2}_j\right)\left(\frac{\left(T^{LPS}_{IN}-T_{OUT_j}\right)+dt^{LPS-2}_j}{2}\right)+\delta\right]^{1/3}}\right\}^{\beta}
\end{aligned}\right] \\
& + \sum_{i\in HPS} C_{cw} q^{cw}_i + k_f\left[C^{Solar}_{cap}+C^{Tank}\right] \\
+H_Y & \left\{\begin{aligned}
&\sum_{f\in F}\left[C^{Fossil}_f \sum_{m\in M}\left(q^{Fossil}_{f,m} D^{sm}_m\right)\right] + \sum_{b\in B}\left[C^{Biofuel}_b \sum_{m\in M}\left(q^{Biofuel}_{b,m} D^{sm}_m\right)\right] + c^{Solar}_{op} \\
&-R^{Solar}\left[\sum_{m\in M}\left(q^{Solar}_m D^{sm}_m\right)\right] - \sum_{m\in M}\sum_{b\in B}\left[R^{Biofuel}_b q^{Biofuel}_{b,m} D^{sm}_m\right] - \sum_{m\in M}\sum_{f\in F}\left[R^{Fossil}_f q^{Fossil}_{f,m} D^{sm}_m\right]
\end{aligned}\right\}
\end{aligned} \tag{1.42}$$

In the previous equation, H_y represents the operating hours per year, K_f is the factor used to annualize the investment and δ is a small value used to avoid infeasibilities. $C^{exc}_{F_{i,j}}$,$C^{cw}_{F_i}$ and $C^{LPS}_{F_j}$ are the fixed charges for exchangers, coolers and heaters, respectively; while the fixed charges for the coolers that exchange heat with the absorption refrigeration system are $C^{ar1}_{F_i}$ and $C^{ar2}_{F_i}$. $C^{exc}_{i,j}$, C^{ar1}_{i}, C^{cw}_{i}, C^{ar2}_{i} and C^{LPS}_{j} are the area cost coefficients for exchangers, $ar1$ coolers, coolers using cooling water, $ar2$ coolers and heaters; while C_{cw} is the unitary cost for the cooling water. C^{Solar}_{cap} and C^{Tank} are the unitary capital costs for the solar collectors and the tank, respectively; besides C^{Fossil}_{f} and $C^{Biofuel}_{b}$ are the unitary costs for the fossil fuels and biofuels, respectively. c^{Solar}_{op} is the annual operational cost for the solar collector. Finally, this objective function considers the revenues obtained by the tax credits due to the reduction in the greenhouse gas emissions; thus R^{Solar}, $R^{Biofuel}_{b}$, and R^{Fossil}_{f} are the unitary tax credits for solar energy, the combustion of biofuels and fossil fuels.

Environmental Objective Function. The environmental objective function is an indirect environmental impact assessment through the overall quantification of the greenhouse gas emissions

$$Min\, nghge^{Overall} = \sum_{m\in M}\sum_{f\in B}\left[GHGE^{Fossil}_{f} q^{Fossil}_{f,m} D^{sm}_{m}\right] + \sum_{m\in M}\sum_{b\in B}\left[GHGE^{Biofuel}_{b} q^{Biofuel}_{b,m} D^{sm}_{m}\right] \tag{1.43}$$

where $nghge^{Overall}$ represents the overall $GHGE$. While, $GHGEGHGE^{Biofuel}_{b}$ and $GHGE^{Fossil}_{f}$ are the unitary $GHGE$ for the fossil f and biofuel b determined through the life cycle analysis (the GREET software was used in this case) given in units of tons of CO_{2eq} reduction per kJ provided.

Social Objective Function. This work considers the social impact associated with the generation of jobs once the project is operating. The generated jobs are determined indirectly for the production of the biofuels and fossil fuels as well as for the operation of the solar collector to satisfy the energy requirements in the system. To carry out this task, the JEDI (jobs and economic development impact) model is used to quantify the number of jobs that can be generated per kWh produced by each energy source (solar collectors, fossil fuels and biofuels). Thus, the social objective function consists in maximizing the generated jobs for the energy produced for fossil fuels, biofuels and the solar collector

$$Max\, njobs^{Overall} = \sum_{m\in M}\sum_{f\in B}\left[NJOB^{Fossil}_{f} q^{Fossil}_{f,m} D^{sm}_{m}\right] + \sum_{m\in M}\sum_{b\in B}\left[NJOB^{Biofuel}_{b} q^{Biofuel}_{b,m} D^{sm}_{m}\right] + \sum_{m\in M}\left[NJOB^{Solar} q^{Solar}_{m} D^{sm}_{m}\right] \tag{1.44}$$

where $NJOB^{Fossil}_{f}$, $NJOB^{Biofuel}_{b}$ and $NJOB^{Solar}$ represent the number of jobs generated per kWh provided by fossil fuels, biofuels and solar collector, respectively.

Finally, once this optimization process is applied the results are shown in Pareto curves that allow considering the trade-offs for the different objectives, and then a specific point of the Pareto curve (the solution to be implemented) must be selected depending on the current degree of preference of the considered objectives. This specific solution determines the configuration and design of the HEN integrated with the AR cycle in addition to the overall sources of energy as well as the characteristics of the solar collector field.

Optimization for the Solar Energy Conservation

Previous step determines the configuration for the heat exchanger network, the capacity of the absorption refrigeration system and the energy requirements, which are obtained on a monthly basis. So, previous step does not consider the variation of the solar radiation during the day, neither the design nor operation of the short-term heat storage subsystem. For this reason, the following optimization process is carried out in an hourly basis.

Initial parameters

The monthly heat load $q^{External}$ of the system is composed of both the process heating requirement and the hot water demand of the AR cycle. This parameter can be calculated knowing the energy provided by the fossil fuels ($q^{Fossil}_{f,m}$), biofuels ($q^{Biofuel}_{b,m}$) and the solar collectors (q^{Solar}_{m}) as $q^{External} = \sum_{f\in F} q^{Fossil}_{f,m} + \sum_{b\in B} q^{Biofuel}_{b,m} + q^{Solar}_{m}, \forall m \in M$.

Since the specific heat capacity, inlet ($T^{Process\_In}$) and outlet ($T^{Process\_Out}$) temperatures of the water circulating in the AR cycle are known (i.e., these are input parameters), the water flow rate can be calculated as $F^{Pro} = \frac{q^{External}}{Cp^{Fluid}(T^{Process\_In} - T^{Process\_Out})}$. On the other hand, the hourly solar energy (solar input for each hour θ) for each month m ($q^{Solar}_{\theta,m}$) is equal to the solar energy collected in each hour per unit of area ($Q^{Useful\_Solar}_{\theta,m}$) multiplied by the area of the solar collector (a^{Solar}_{c}) and a conversion factor (D^{sh}) as follows ($q^{Solar}_{\theta,m} = Q^{Useful\_Solar}_{\theta,m}\ a^{Solar}_{c} \frac{1}{D^{sh}}, \forall \theta \in \Theta, m \in M$).

Optimization of the solar energy conservation

Cold Water Tank. The cold storage tank at the exit of the absorption refrigeration cycle is required to provide the residence time to the heat-transfer fluid and, at the same time, to allow a variable flow rate entering to the solar collectors to maintain the outlet temperature of the solar field below the saturation temperature (100°C at 1 bar to avoid operational problems). In this unit, the inlet flow rate, inlet and outlet temperatures are constant, so only the mass balances need to be modeled. The water accumulation in the cold storage tank at different hours for $\theta > 1$ ($sa^{WT}_{\theta,m}$) is equal to the previous accumulation $sa^{WT}_{\theta-1,m}$ plus the flow rate entering to the tank F^{Pro} minus the flow rate exiting from the tank $f^{WT\_Out}_{\theta,m}$ at any hour θ

$$sa^{WT}_{\theta,m} = sa^{WT}_{\theta-1,m} + F^{Pro} - f^{WT\_Out}_{\theta,m}, \forall \theta > 1, m \in M \tag{2.1}$$

For the first period, this equation is stated as $sa^{WT}_{\theta,m} = sa^{WT\_Initial}_{0} + F^{Pro} - f^{WT\_Out}_{\theta,m}, \forall \theta = 1, m \in M$, and to guarantee the continuity of the cycles, a necessary condition is that the initial accumulation must be equal to the last accumulation for any day of any month (i.e., $sa^{WT\_Initial}_{0} = sa^{WT}_{\theta,m}, \forall \theta = 24, m \in M$).

Splitter Div-1. The mass balance for the splitter at the exit of the storage tank Div-1 establishes that at any hour θ for each month m, the outlet flow rate ($f^{WT\_Out}_{\theta,m}$) is equal to the flow rate sent to the solar collector ($f^{Coll}_{\theta,m}$) plus the bypassing flow rate sent to Mix-2 ($f^{By}_{\theta,m}$)

$$f^{WT\_Out}_{\theta,m} = f^{Coll}_{\theta,m} + f^{By}_{\theta,m}, \forall \theta \in \Theta, m \in M \tag{2.2}$$

Solar Collector. The energy supplied by the solar collector ($q^{Solar}_{\theta,m}$) at any period of time θ of each month m increases the inlet temperature ($T^{Process\_Out}$) to the outlet temperature ($t_{\theta,m}^{Solar}$) of the liquid water, and this is modeled as follows

$$f_{\theta,m}^{Coll} Cp^{Fluid} \left(t_{\theta,m}^{Solar} - T^{Process\_Out} \right) = q_{\theta,m}^{Solar}, \forall \theta \in \Theta, m \in M \quad (2.3)$$

To avoid the vaporization of the heat transfer fluid (i.e., water), the outlet temperature $t_{\theta,m}^{Solar}$ must be lower than the boiling temperature (i.e., $T_{\theta,m}^{Solar\_Out} \leq T^{Vaporization}$).

Splitter Div-2

The flow rate coming from the solar collector ($f_{\theta,m}^{Coll}$) is segregated to be sent to the hot tanks ($f_{p,\theta,m}^{Tank\_In}$) or sent directly to the process bypassing the storage system ($f_{\theta,m}^{TankBy}$)

$$f_{\theta,m}^{Coll} = \sum_{p \in P} f_{p,\theta,m}^{Tank\_In} + f_{\theta,m}^{TankBy}, \forall \theta \in \Theta, m \in M \quad (2.4)$$

Multitank TES System. During the useful hours of solar radiation, the captured solar energy can be higher than the energy demanded by the AR cycle. The excess heat is stored in a multitank sensible energy storage system that uses liquid water as both the heat-transfer fluid and the storage media. For short-term periods when solar radiation is not available, the hot water from the storage tanks can provide heating to the AR cycle without the need to burn fossil fuels or biofuels.

The accumulation in the tank p at any period different to the 1 (i.e., the first hour of the day) and for any month m ($sa_{p,\theta,m}^{Tank}$) is equal to the accumulation in the previous period s $a_{p,\theta-1,m}^{Tank}$ plus the flow rate entering to the tank in this period $f_{p,\theta,m}^{Tank\_In}$ minus the flow rate leaving the tank p $f_{p,\theta,m}^{Tank\_Out}$ at period θ

$$sa_{p,\theta,m}^{Tank} = sa_{p,\theta-1,m}^{Tank} + f_{p,\theta,m}^{Tank\_In} - f_{p,\theta,m}^{Tank\_Out}, \forall p \in P, \theta > 1, m \in M \quad (2.5)$$

For the first period, the initial accumulation is given as $sa_{p,0}^{Tank\_Initial}$ and the same equation apply. Furthermore, the initial and final conditions must be the same (i.e., $sa_{p,0}^{Tank\_Initial} = sa_{p,\theta=24,m}^{Tank}, \forall p \in P, m \in M$).

In addition, each term of the mass balance equations is multiplied by the specific heat capacity and the corresponding temperature to obtain the following energy balances

$$\begin{aligned} sa_{p,\theta,m}^{Tank} Cp^{Fluid} t_{p,\theta,m}^{Tank} &= sa_{p,\theta-1,m}^{Tank} Cp^{Fluid} t_{p,\theta-1,m}^{Tank} \\ &+ f_{p,\theta,m}^{Tank\_In} Cp^{Fluid} t_{\theta,m}^{Solar\_Out} - f_{p,\theta,m}^{Tank\_Out} Cp^{Fluid} t_{p,\theta,m}^{Tank} \\ &- q_{p,\theta,m}^{Loss}, \forall p \in P, \theta > 1, m \in M \end{aligned} \quad (2.6)$$

where $q_{p,\theta,m}^{Loss}$ represents the energy losses during the period θ in the tank p for the month m. It should be noted that this term depends on the material, type of insulating and size for the tank, and it has significant variations throughout day because of the changes in the ambient temperatures. Previous relationship is nonconvex because this has bilinear terms (flow rates or stored material times temperatures). Furthermore, the initial temperature must be equal to the final temperature ($t_{p,0}^{Tank\_Initial} = t_{p,\theta=24,m}^{Tank}, \forall p \in P, \theta=24, m \in M$).

Mixer Mix-1. After the multitank TES system, it is located a mixer to combine the flow rates leaving all the tanks with the flow rate sent directly to this unit (bypassing stream). The flow rate leaving the tank p ($f_{p,\theta,m}^{Tank\_Out}$) is mixed with the bypass flow rate ($f_{\theta,m}^{TankBy}$) obtaining the mixed flow rate ($f_{\theta,m}^{Mix}$)

$$\sum_{p \in P} f_{p,\theta,m}^{Tank\_Out} + f_{\theta,m}^{TankBy} = f_{\theta,m}^{Mix}, \forall \theta \in \Theta, m \in M \quad (2.7)$$

Then, the associated energy balance for Mix-1 can be evaluated as the product of each term of the mass balance times the specific heat capacity and corresponding temperature

$$\begin{aligned} &\sum_{p \in P} f_{p,\theta,m}^{Tank\_Out} Cp^{Fluid} t_{p,\theta,m}^{Tank} + f_{\theta,m}^{TankBy} Cp^{Fluid} t_{\theta,m}^{Solar\_Out} \\ &= f_{\theta,m}^{Mix} Cp^{Fluid} t_{\theta,m}^{Mix}, \forall \theta \in \Theta, m \in M \end{aligned} \quad (2.8)$$

in the previous relationship several bilinear terms appear for the products between flow rates times temperatures.

Mixer Mix-2. In this mixer, the bypass flow rate coming from the splitter Div-1 is mixed with $f_{\theta,m}^{Mix}$, which is the flow rate at the exit of the first mixer, and its mass and energy balances are stated as follows

$$f_{\theta,m}^{Mix} + f_{\theta,m}^{By} = F_{\theta,m}^{Pro}, \forall \theta \in \Theta, m \in M \quad (2.9)$$

$$\begin{aligned} &f_{\theta,m}^{Mix} Cp^{Fluid} t_{\theta,m}^{Mix} + f_{\theta,m}^{By} Cp^{Fluid} T^{Process\_Out} \\ &= F_{\theta,m}^{Pro} Cp^{Fluid} t_{\theta,m}^{Heater}, \forall \theta \in \Theta, m \in M \end{aligned} \quad (2.10)$$

Also, in previous relationship appear bilinear terms for the products between flow rates times temperatures.

Heater. The hybrid energy system under study requires backup provisions such as biofuels and/or fossil fuels in addition to solar energy storage to meet the heating demands of the AR generator during periods of low or zero solar radiation. Therefore, it is necessary to determine the optimal combination of backup fuels (i.e., how much of each type of backup fuel must be used) considering the unit price as well as the unit environmental impact and availability throughout the year of each backup resource. Next, the energy balance in the heater states that if the entering temperature to the heater is lower than the inlet temperature required in the AR cycle ($t_{\theta,m}^{Heater} < T^{Process\_In}$), then the heater must provide the energy to reach it, which is modeled as follows

$$F^{Pro} Cp^{Fluid} \left(T^{Process\_In} - t_{\theta,m}^{Heater} \right) = q_{\theta,m}^{Heater}, \forall \theta \in \Theta, m \in M \quad (2.11)$$

The energy used by the heater at any period θ for each month m is supplied by fossil fuels and/or biofuels, and this is modeled as follows

$$\begin{aligned} q_{\theta,m}^{Heater} &= \sum_{f \in F} f_{f,\theta,m}^{Fossil} Heating_f^{Power} \alpha_f^{Fossil} \\ &+ \sum_{b \in B} f_{b,\theta,m}^{Biofuel} Heating_b^{Power} \alpha_b^{Biofuel}, \forall \theta \in \Theta, m \in M \end{aligned} \quad (2.12)$$

In the previous equation, $Heating_f^{Power}$ and $Heating_b^{Power}$ represent the heating power of the fossil fuel f and biofuel b, respectively; while α_f^{Fossil} and $\alpha_b^{Biofuel}$ are the combustion efficiencies for fossil fuels and biofuels, respectively.

Additional Constraints

Maximum availability of biofuels

Usually the availability of biofuels is seasonally limited; consequently, the model considers this restriction as follows

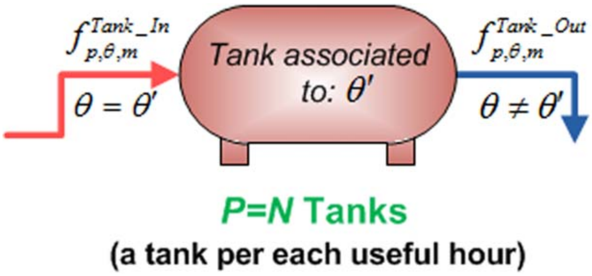

Figure 5. Representation of tanks storing at period $\theta=\theta'$ and dispatching at periods $\theta \neq \theta'$.

[Color figure can be viewed in the online issue, which is available at wileyonlinelibrary.com.]

$$\left(D_m^{dm} D^{sh}\right) \sum_{\theta \in \Theta} f_{b,\theta,m}^{Biofuel} \leq Avail_{b,m}^{Max}, \forall b \in B, m \in M \quad (2.13)$$

where D_m^{dm} and D^{sh} are useful parameters to adjust the time units.

Maximum accumulation in the multitank TES system

To determine the volume and cost of the hot tanks placed in the TES system, the maximum accumulation in each tank for all periods θ and months m must be computed as follows

$$sa_{p,\theta,m}^{Tank} \leq sa_p^{Tank\_Max}, \forall p \in P, \theta \in \Theta, m \in M \quad (2.14)$$

Storage tank volumes

The volume of each hot tank (v_p^{Tank}) in the TES system can be estimated as the product of the maximum accumulation ($sa_p^{Tank\_Max}$), and the average residence time ($\tau_{average}^{residence}$) divided by the density of the heat transfer fluid (ρ^{Fluid})

$$v_p^{Tank} = sa_p^{Tank\_Max} \frac{\tau_{average}^{residence}}{\rho^{Fluid}}, \forall p \in P \quad (2.15)$$

Existence of the tanks

To determine the existence of a given tank p in the optimal configuration, a binary variable (y_p) is used and activated through the following relationship:

$$sa_p^{Tank\_Max} \leq SA^{Up} y_p, \forall p \in P \quad (2.16)$$

where SA^{Up} is the maximum capacity for the storage tanks. The binary variable y_p is used to determine the fix part of the capital cost of the storage tanks.

Cost of storage tanks

The cost of each tank ($cost_p^{Tank}$) is calculated as follows

$$cost_p^{Tank} = K_f \left[FC^{Tank} y_p + VC^{Tank} \left(v_p^{Tank} \right)^{\beta^{Tank}} \right], \forall p \in P \quad (2.17)$$

where K_f is a factor used to annualize the investment, FC^{Tank} and VC^{Tank} are the fixed and variable unit capital costs, respectively; while y_p is the binary variable associated with the existence of the tank p, and finally β^{Tank} represents an exponent to consider the economies of scale.

Similarly to the hot tanks, constraints for the cold water tank to evaluate its maximum accumulation ($sa_{\theta,m}^{WT} \leq sa^{WT\_Max}$, $\forall \theta \in \Theta, m \in M$), volume $\left(v^{WT} = sa^{WT\_Max} \frac{\tau_{average}^{residence}}{\rho^{Fluid}} \right)$ and cost $\left(cost^{WT} = K_f \left[FC^{Tank} + VC^{Tank} (v^{WT})^{\beta^{Tank}} \right] \right)$ are required.

Operation of the tank

The aforementioned constraints include mass and energy balances as well as availability constraints of biofuels and cost functions for the scheme shown in Figure 4; however, the operation of the tanks has not been described yet. In this sense, during the sunlight hours (considering N hours of solar radiation) the hot tanks can receive hot water at different temperatures from the solar collector. During demand, if hot water from a storage tank is discharged and, at the same time, hot water from solar collectors is supplied to the tank, the temperature of the water inside the storage tank and leaving the tank will vary with respect to time. The detailed model of this dynamic operation involves one differential equation per hot tank. Even for a short-horizon (i.e., a day), a limitation of this approach is that the size of the detailed model complicates the problem, because of the increase in the computation required to obtain the solution. To overcome this limitation, this article proposes four different options to simulate the operation of the hot tanks that are described as follows

Case A. Tanks storing at period $\theta=\theta'$ and dispatching at periods $\theta \neq \theta'$

In this option, each hot tank can store the heat-transfer fluid coming from the solar collectors at a specific hour (θ') and can dispatch in the rest of the hours (see Figure 5). Then, a tank must be associated with each useful hour of solar radiation; as consequence, this configuration requires N tanks to store the excess heat from the solar radiation. The aforementioned operation is modeled through the following equations:

$$f_{p,\theta,m}^{Tank\_In} = 0, \forall p \neq \theta', m \in M \quad (2.18)$$

$$f_{p,\theta,m}^{Tank\_Out} = 0, \forall p = \theta', m \in M \quad (2.19)$$

Case B. Tanks storing at period $\theta \neq \theta'$ and dispatching at period $\theta=\theta'$

As can be seen in Figure 6, this type of tank operation implies that each tank can dispatch at period θ' and store over a period of time different to θ'. Similarly to previous option, this case demands the possible existence of N tanks (a tank per period), and then the next constraints must be added

$$f_{p,\theta,m}^{Tank\_In} = 0, \forall p = \theta', m \in M \quad (2.20)$$

$$f_{p,\theta,m}^{Tank\_Out} = 0, \forall p \neq \theta', m \in M \quad (2.21)$$

Case C. Combination of options A and B

This alternative consists of a combination of the aforementioned cases, where a set of tanks can store at period

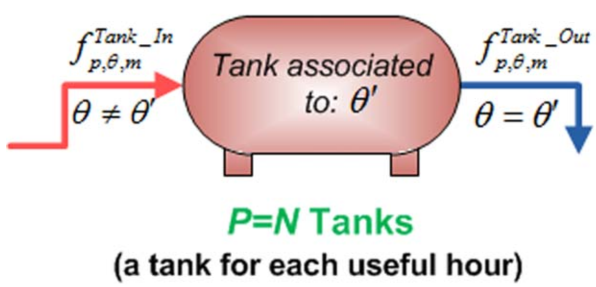

Figure 6. Representation of tanks storing at period $\theta \neq \theta'$ and dispatching at period $\theta=\theta'$.

[Color figure can be viewed in the online issue, which is available at wileyonlinelibrary.com.]

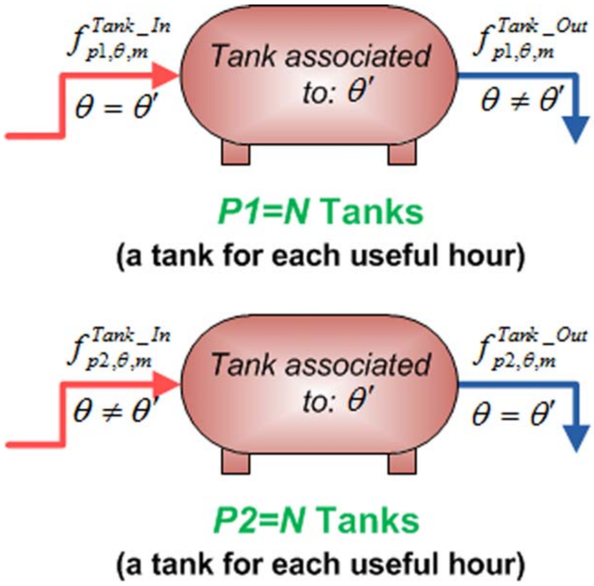

Figure 7. Representation of the combination of two operation modes of the hot tanks.

[Color figure can be viewed in the online issue, which is available at wileyonlinelibrary.com.]

$\theta=\theta'$ and dispatch at period $\theta \neq \theta'$; also, other set of tanks can collect hot water at period $\theta \neq \theta$ and the water from the tanks is discharged only at period $\theta=\theta'$ (see Figure 7). Hence, for this option the subset $p1$ represents the set of tanks storing at period $\theta=\theta'$ and dispatching at period $\theta \neq \theta'$, while the subset $p2$ contains the set of tanks collecting at period $\theta \neq \theta'$ and dispatching at period $\theta=\theta'$. This is modeled as follows

$$f_{p,\theta,m}^{Tank\_In}=0, \forall p1 \neq \theta', m \in M \tag{2.22}$$

$$f_{p,\theta,m}^{Tank\_In}=0, \forall p2=\theta', m \in M \tag{2.23}$$

$$f_{p,\theta,m}^{Tank\_Out}=0, \forall p1=\theta', m \in M \tag{2.24}$$

$$f_{p,\theta,m}^{Tank\_Out}=0, \forall p2 \neq \theta', m \in M \tag{2.25}$$

Case D. Disjunctive model

Finally, in this option hot water can pass from the solar collectors to the storage tanks and hot water can leave the storage tanks at any time that it is required; however, these two operations can never occur at the same time (see Figure 8). Then, the following disjunction establishes that if the Boolean variable $Z_{p,\theta,m}$ is true, then the tank only can store the heat-transfer fluid; otherwise, if the Boolean variable is false, it means that only the outlet flow rate can be possible

$$\begin{bmatrix} Z_{p,\theta,m} \\ f_{p,\theta,m}^{Tank\_Out}=0 \end{bmatrix} \vee \begin{bmatrix} \neg Z_{p,\theta,m} \\ f_{p,\theta,m}^{Tank\_In}=0 \end{bmatrix}, \forall p \in P, \theta \in \Theta, m \in M$$

In previous disjunction, the Boolean variables $Z_{p,\theta,m}$ are converted into a set of binary variables $z_{p,\theta,m}$ to carry out the reformulation of the disjunctive model obtaining the next algebraic equations

$$f_{p,\theta,m}^{Tank\_In} \leq F^{Up} z_{p,\theta,m}, \forall p \in P, \theta \in \Theta, m \in M \tag{2.26}$$

$$f_{p,\theta,m}^{Tank\_Out} \leq F^{Up}\left(1-z_{p,\theta,m}\right), \forall p \in P, \theta \in \Theta, m \in M \tag{2.27}$$

where F^{Up} is an upper limit for the inlet and outlet flow rates in the tanks. Notice also that the number of binary variables increases exponentially when the number of tanks considered (p) increases.

Objective function for the design and operation of the solar energy conservation

The economic objective function consists in minimizing the total annual cost (tac), which is composed by the storage hot tanks system cost, in addition to the cold water tank cost, as well as the costs generated by the consumption of fossil fuels and biofuels required to satisfy the backup energy demanded by the AR cycle

$$Min\, tac=\sum_{p \in P} cost_p^{Tank}+cost^{WT}+D^{sh}\left(D_m^{dm}\right)\sum_{\theta \in \Theta}\sum_{m \in M} \left(\sum_{b \in B} Cost_b^{Biofuel} f_{b,\theta,m}^{Biofuel}+\sum_{f \in F} Cost_f^{Fossil} f_{f,\theta,m}^{Fossil}\right) \tag{2.28}$$

In previous objective function, D^{sh} and D_m^{dm} are conversion factors to annualize the fuel costs; whereas $Cost_b^{Biofuel}$ and are the unitary costs for biofuel b, and fossil fuel f, respectively.

Results

To show the applicability of the proposed formulation, this work considers two case studies. In this sense, the following parameters are fixed for the presented examples:

- The location considered for the examples is Morelia, México, which has the coordinates N 19° 42′ 08″ and W 101° 11′ 08″.
- The values for the parameters H_Y, K_f and β^{Tank} used are 8,760 h/year, 1 year^{-1} and 1, respectively.
- The coefficients of operation for the absorption refrigeration cycle (COP^{ar2}) and the steam system (COP^{LPS}) are 0.7 and 0.95, respectively.[72–75]
- The inlet and outlet temperatures of the cold external utility for the coolers cw and $ar1$ are: $T_{IN}^{cw}=30$°C, $T_{OUT}^{cw}=40$°C; and $T_{IN}^{ar1}=50$°C, $T_{OUT}^{ar1}=$ 80°C.
- The unitary cost for the cold utility C_{cw} is \$10/(year K).
- The number of jobs generated by the solar collectors is 9.95459×10^{-10} Jobs/kWh.
- The water inlet and outlet temperatures of the absorption refrigeration system are 50°C and 80°C, respectively.
- The unitary fixed part of the capital cost for the tanks is \$1,200, while the unitary variable part for the capital cost of the tanks is \$520/m^3.

For the energy integration of the HEN and the AR system two solar collectors (Parabolic trough solar collector -PTSC and Evacuated tube solar collector -ETSC) are considered.

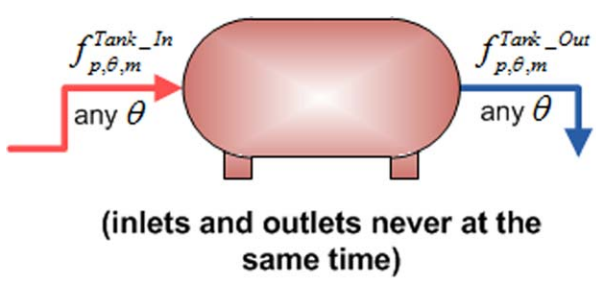

Figure 8. Representation of tanks storing and dispatching at any hour, but never at the same time.

[Color figure can be viewed in the online issue, which is available at wileyonlinelibrary.com.]

Table 1. Useful Collected Energy per Month for Different Solar Collectors[76]

Month/Type of Solar Collector	PTSC [kJ/(m^2 month)]	ETSC [kJ/(m^2 month)]
January	409,293	245,576
February	443,016	265,810
March	577,530	346,518
April	571,860	343,116
May	555,768	333,461
June	454,410	272,646
July	443,610	266,166
August	439,425	263,655
September	394,470	236,682
October	410,967	246,580
November	407,430	244,458
December	522,288	235,030

Table 1 shows the useful collected energy per month per unit area of solar collector for PTSC and ETSC. In addition, for designing the multitank TES subsystem Table 2 presents the useful energy for each sunlight hour per square meter of area in Morelia, México.[76–80] Table 2 also shows the number of tanks assigned to each hour of solar radiation (useful for Cases A, B and C); for example, in Case A the Tank 1 can only receive the heat-transfer fluid from 6:00 am to 7:00 am and dispatch in the rest of the day, while the Tank 12 is able to receive hot water from 5:00 pm to 6:00 pm and send it to the AR cycle at the rest of the time. On the other hand, for Case B, the Tank 1 can only dispatch from 6:00 am to 7:00 am and the heat transfer fluid is received in the rest of the day.

The fuels and biofuels taken into account in the examples presented are shown in Table 3 as well as their heating power, overall unitary *GHGE*, unitary cost and unitary number of jobs created by each fuel considered, while Table 4 shows the maximum amount monthly available of each fuel.

All the problems were implemented in the general algebraic modeling system (GAMS) using the solver DICOPT in conjunction with the solvers CONOPT and CPLEX to solve the associated MINLP, NLP and MILP problems.[81] It should be noted that the nonlinear terms included in the first stage of optimization are in the economic objective function (in the part associated with the capital cost for the heat-transfer units), while the second stage contains nonlinear terms in all energy balances considered (representing bilinear terms for the flow rates times the temperatures). For solving this problem the following initialization procedure has been implemented. First the model without considering the nonlinear part of the capital cost for the heat transfer units was solved (this is a mixed-integer linear problem), then this is used as initial guess for the nonlinear mixed-integer problem. For solving the second stage, the discretization approach proposed by Rubio-Castro et al.[82] was used first to provide initial guesses for the mixed-integer nonlinear problem. It should be noticed that global optimization solvers can be used to identify global optimal solutions; however, there are required appropriate limits for the variables involved in the nonconvex terms, and because the number of nonconvex terms involved in the model, this task can consume a considerable CPU time.

Example 1

A pharmaceutical plant is installed in Morelia; this industry has three hot process streams and two cold process streams to carry out the energy integration. The data for the process streams is contained in Table 5.

Once the energy integration (step 1) was applied for this example; it generates the results shown in Figure 9. As it can be seen, the results are represented through the Pareto curve obtained comparing the *TAC* and the overall *GHGE*, evaluating the number of jobs for each point. In the Pareto curve, points A, B and C can be identified, where point A represents the optimal solution for the lowest overall *GHGE*, being zero for this concrete solution. Otherwise, point B is the best economic solution. Additionally, a balanced solution can be identified in Figure 9, which is point C, because it represents a good number of generated jobs (2,574) and, at the same time, both *TAC* and *GHGE* can be considered acceptable (*TAC* of \$1,135,388.10/year and overall *GHGE* of 1,500 tons $CO_{2\ eq.}$/year). Thus, point C is the solution selected to apply the solar energy conservation (step 2), which considers a PTSC of 15,321.82 m^2. Additionally, the AR cycle requires 3,712.03 kJ/s. The configuration of the HEN obtained is shown in Figure 10; in this solution there are two heat exchanger units between process streams and cooling water is not required. Figure 11 illustrates the type of energy source required per month.

Thus, the required flow rate to run the absorption refrigeration cycle is $F^{Pro}=29.573 kg/s$. The four cases for the operation of the storage tanks were considered and the results are presented as follows.

Case A. Tanks storing at period $\theta = \theta'$ and dispatching at periods $\theta \neq \theta'$

In this case a potential hot tank is considered for each hour of the day with sunlight (each tank allows receiving hot water during a sunlight hour and dispatches in the rest of the day). Since Morelia has 12 h with solar radiation (see Table 2) and 12 h without it, then it is considered the possible existence of

Table 2. Useful Collected Energy per Hour for an Average Day of each Month in Morelia, México-Given in kJ/(m^{2}h)[76–80]

Tank	Hour/month	Jan	Feb	Mar	Apr	May	Jun	Jul	Aug	Sep	Oct	Nov	Dec
1	06:00 am	0	0	0	0	0	102	14	0	0	0	0	0
2	07:00 am	0	0	0	44	173	615	498	54	0	0	0	293
3	08:00 am	311	401	729	914	899	1,140	1,023	483	378	436	1,045	1,013
4	09:00 am	595	1,056	1,405	1,632	1,356	1,409	1,341	967	517	1,208	1,277	1,386
5	10:00 am	1,320	1,521	1,795	1,959	1,703	1,613	1,535	1,369	1,399	1,477	1,532	1,360
6	11:00 am	1,450	1,605	1,847	2,024	1,876	1,741	1,687	1,557	1,553	1,544	1,509	1,306
7	12:00 pm	1,398	1,669	1,873	2,154	2,002	1,754	1,714	1,678	1,637	1,510	1,416	1,333
8	1:00 pm	1,476	1,711	1,900	2,111	2,066	1,741	1,700	1,691	1,651	1,494	1,439	1,413
9	2:00 pm	1,527	1,753	1,951	2,132	2,050	1,652	1,618	1,718	1,637	1,510	1,486	1,466
10	3:00 pm	1,605	1,817	2,082	1,980	2,003	1,472	1,383	1,624	1,580	1,510	1,532	1,440
11	4:00 pm	1,683	1,838	2,108	1,828	1,766	1,114	1,078	1,463	1,399	1,393	1,439	1,040
12	5:00 pm	1,501	1,690	1,977	1,523	1,388	794	719	1,074	895	1,175	906	586
	6:00 pm	337	761	963	761	646	0	0	497	503	0	0	0

Table 3. Data for the Fossil Fuels and Biofuels Considered in the Examples

#	Fuel	Heating power [kJ/kg]	Overall *GHGE* [ton CO^2 eq/kJ]	Cost [$/mm kJ]	Generation of Jobs [Jobs/kJ]
Fossil Fuels					
1.	Coal	35,000	2.21357×10^{-7}	1.5559	1.06281×10^{-11}
2.	Oil	45,200	8.05408×10^{-8}	18.2447	1.81677×10^{-11}
3.	Natural Gas	54,000	7.90892×10^{-8}	5.8349	5.25431×10^{-11}
Biofuels					
1.	Biomass	17,200	2.44307×10^{-8}	2.0303	6.6964×10^{-8}
2.	Biogas	52,000	2.68216×10^{-8}	8.5388	5.25431×10^{-7}
3.	Softwood	20,400	3.3482×10^{-8}	2.5332	1.46691×10^{-8}
4.	Hardwood	18,400	3.3482×10^{-8}	2.8975	5.43641×10^{-8}
5.	Biodiesel	40,200	5.13283×10^{-8}	31.3092	2.46582×10^{-6}
6.	Bioethanol	29,600	5.8436×10^{-8}	14.4212	2.87453×10^{-6}

Table 4. Monthly Amount Available for the Fossil Fuels and Biofuels (kg/month)

Fuel/month	Jan	Feb	Mar	Apr	May	Jun	Jul	Aug	Sep	Oct	Nov	Dec
Biomass	10,000	10,000	40,000	50,000	70,000	150,000	100,000	50,000	40,000	40,000	30,000	20,000
Biogas	5,000	5,000	6,000	6,500	6,500	10,000	10,000	10,000	8,000	7,000	6,000	5,000
Softwood	30,000	30,000	25,000	25,000	23,000	23,000	15,000	15,000	20,000	25,000	25,000	30,000
Hardwood	30,000	30,000	25,000	25,000	23,000	23,000	15,000	15,000	20,000	25,000	25,000	30,000
Biodiesel	5,000	5,500	6,000	7,000	10,000	10,000	10,000	10,000	9,000	8,000	7,000	6,000
Bioethanol	10,000	11,000	12,000	12,000	15,000	15,000	15,000	15,000	14,000	13,000	11,000	10,000

12 tanks in the multitank TES system, in addition to the water tank used to store the cold water entering to the solar collector. All the tank sizes are optimized accounting for the optimal operation and minimizing the total annual cost. Table 6 contains the size of the hot tanks involved in the optimal solution of this case. It should be noted that the Tank 1 is not required (which corresponds to the tank receiving from 6:00 am to 7:00 am and dispatching in the rest of the time), while the volume of Tank 12 is much smaller compared to rest of tanks. Moreover, the maximum accumulation for each tank has a linear correspondence respect to the tank volume; also, the cold water tank requires a large volume (almost 700 m^3) to provide a variable flow rate entering the solar collectors. Finally, the *TAC* for the energy storage system is $901,797.49/year.

Case B. Tanks storing at periods $\theta \neq \theta'$ and dispatching at period $\theta = \theta'$

In this case 12 tanks dispatching at a specific hour and receiving in the twenty three remaining hours were considered. However, no feasible solution was obtained for this case, even for a special case that considers 24 tanks.

Case C. Combination

This case includes a combination of each type of tanks previously described (Case A and Case B), where 12 tanks receive at period $\theta = \theta'$ and dispatch at interval $\theta \neq \theta'$, while other 12 tanks receive at periods $\theta \neq \theta'$ and dispatch at period $\theta = \theta$ during the sunlight hours. Table 7 shows the tanks required in the solution as well as their optimal size. The optimal sizes for the Tanks 4, 11 and 12 are similar to Case A. Furthermore, Table 7 shows the results for this case.

Table 5. Streams Data for Example 1

Stream	Inlet temperature [°C]	Outlet temperature [°C]	*FCp* [kW/°C]
H1	125	65	38.75
H2	85	25	18.75
H3	45	25	43.75
C1	35	240	20
C2	35	55	36.25

It should be noted that the storage tanks operating as Case B are not required in the optimal solution. Additionally, the tank that stores at interval 6:00am–7:00 am is not needed. Notice that this solution is similar to the results obtained for Case A (owing to the optimal solution for Case C also considers 11 storage tanks operating as Case A); however, in Case C the tank costs are reduced significantly ($901,797.49/year vs. $837,266.56/year for cases A and C, respectively).

Case D. Disjunctive model

Table 8 contains the optimal number of tanks required by the solution (where only nine tanks are required) as well as their sizes. It should be noted that in this operation mode, hot water can flow into and out of the storage tanks at any time but not at the same time. As can be seen, three tanks have volumes higher than 100 m^3; however, the size of the other tanks is significantly smaller respect to Cases A and C. For this reason, the total annual cost is also lower than those of previous cases. In this case, the total annual cost of the TES system is $738,296.76/year.

Finally, Table 9 contains a comparison for the three analyzed cases in this example. Notice that Cases A and C require more tanks than Case D; so, Case D is the solution with the lowest total annual cost. Notice also that the cost and, consequently, the volume of the cold water tank is the

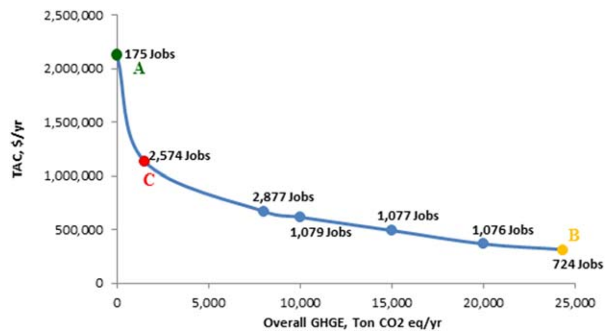

Figure 9. Pareto curve for Example 1.

[Color figure can be viewed in the online issue, which is available at wileyonlinelibrary.com.]

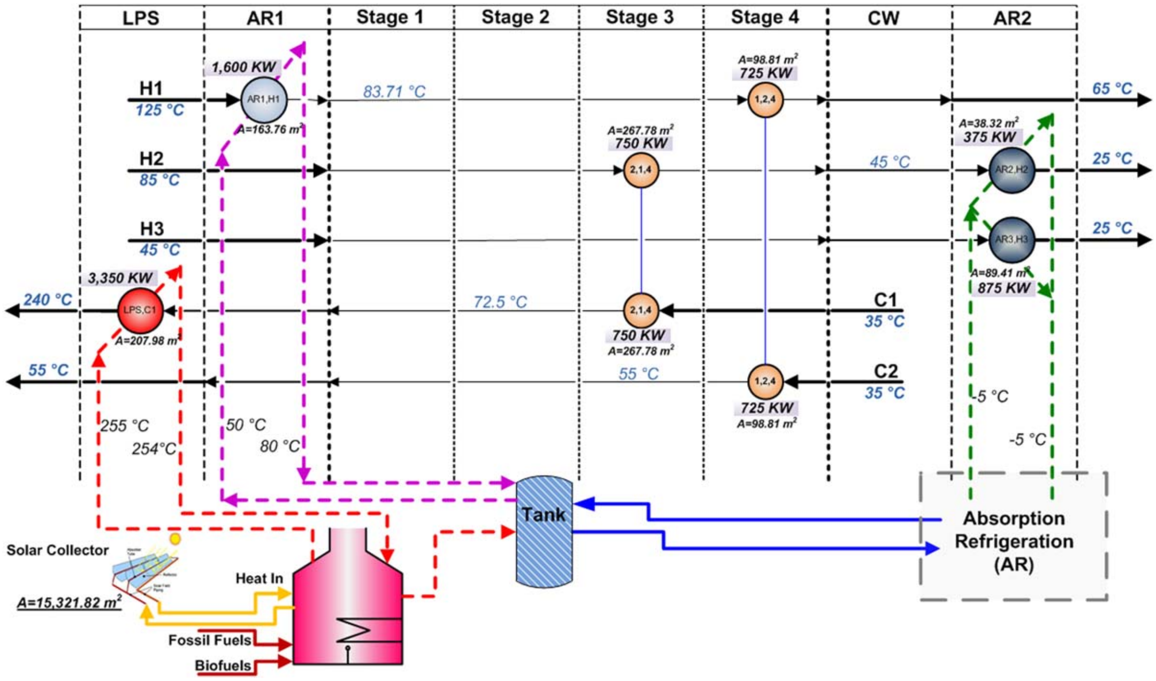

Figure 10. Configuration of the integrated HEN and AR for Example 1.

[Color figure can be viewed in the online issue, which is available at wileyonlinelibrary.com.]

same in the three cases; thus, the cost differences between these solutions are due to the different costs of the multitank TES systems. According to the tanks operation mode, Case D offers the best economic solution; however, an important quantity of binary variables must be included in the formulation (i.e., this case is the more difficult to solve). Thus, Case C reduces 7.16% the total annual cost respect to Case A; while Case D decreases the total annual cost in 18.13% compared with Case A and 11.82% respect to Case C. So, the results show that the best configuration minimizes the number of required tanks. Also, the total annual cost is obtained when the flow rate entering and the flow rate exiting the tanks are permitted at any time (Case D). However, the optimal configurations obtained for Cases A, B and C are included to consider different modes of operation, which can be useful when there are special requirements.

Note that the internal flow rates, temperatures and accumulations of the proposed configuration are determined for each case considering their variation during the day and months.

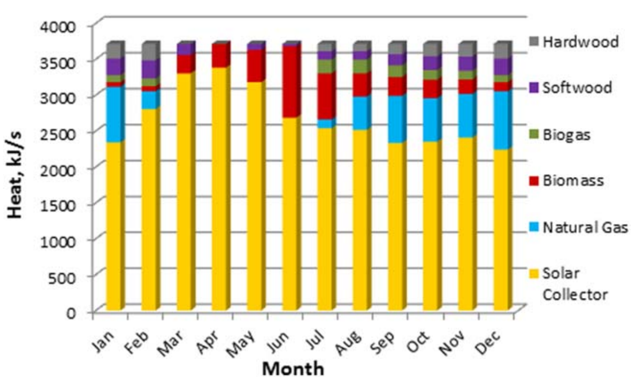

Figure 11. Energy sources required for each month in Example 1.

[Color figure can be viewed in the online issue, which is available at wileyonlinelibrary.com.]

Example 2

This example considers a formic acid process, which has six hot process streams and four cold process streams. Table 10 shows the inlet and target temperatures for the process streams as well as the product of the flow rate times the heat capacity to carry out the energy integration and synthesis of the HEN and AR system.

From the Pareto front given by the first step of the optimization process (see Figure 12) can be identified the points A, B and C, where point A corresponds to the optimal solution for the minimum overall *GHGE* and maximum *TAC*, while the point B is the optimal solution for the minimum *TAC* and maximum overall *GHGE*. As it can be seen in Figure 12, neither the point A nor the point B involves an acceptable number of jobs (459 and 707 jobs, respectively). Then, the best solutions for the creation of jobs are the points with overall *GHGE* values of 10,000 tons $CO_{2\ eq}$/yr, 20,000 tons $CO_{2\ eq}$/yr and 30,000 tons $CO_{2\ eq}$/yr (3,699, 3,580 and 3,484 jobs, respectively). Between these three alternatives, point C was selected to apply the next optimization process (step 2), which has a great number of jobs and an appropriate overall

Table 6. Solution for Case A of Example 1

Tank	Maximum Accumulation [kg/s]	Volume [m^3]	Cost [$]
2	5.45	19.62	11,400.07
3	28.67	103.20	54,861.53
4	22.11	79.60	42,591.55
5	26.57	95.65	50,938.79
6	35.68	128.46	68,000.79
7	34.40	123.85	65,601.45
8	33.30	119.89	63,544.87
9	32.14	115.72	61,374.03
10	37.39	134.62	71,199.92
11	22.47	80.92	43,277.07
12	1.85	6.65	4,659.06
Cold water tank	193.99	698.36	364,348.38

Table 7. Solution for Case C of Example 1

Tank	Maximum Accumulation [kg/s]	Volume [m^3]	Cost [$]
Tanks operating as Case A			
2	21.26	76.54	40,998.65
3	15.46	55.65	30,137.81
4	22.11	79.60	42,591.55
5	24.95	89.80	47,897.39
6	26.09	93.92	50,037.46
7	25.20	90.73	48,380.44
8	36.43	131.15	69,396.60
9	24.61	88.61	47,275.98
10	25.14	90.51	48,266.19
11	22.47	80.92	43,277.07
12	1.85	6.65	4,659.06
Cold water tank	193.99	698.36	364,348.38

Table 8. Solution for Case D of Example 1

Tank	Maximum Accumulation [kg/s]	Volume [m^3]	Cost [$]
1	13.24	47.67	25,986.56
2	13.21	47.57	25,934.19
3	6.23	22.44	12,868.24
4	45.32	163.15	86,036.97
5	13.99	50.37	27,391.46
6	31.69	114.08	60,523.12
7	30.03	108.11	57,418.56
8	18.59	66.92	35,996.56
9	21.68	78.06	41,792.72
Cold water tank	193.99	698.36	364,348.38

GHGE. Figure 13 shows the configuration for the heat exchanger network as well as the general scheme for the energy sources to run the absorption refrigeration cycle. This solution requires a PTSC to provide the energy demanded by the AR cycle, which has an area of 31,056 m^2, in addition to fossil fuels and biofuels that are also needed to supply the heating load of the overall system. The total heat load of the absorption refrigeration cycle is 13,960 kJ/s. Figure 14 shows the types of energy sources required in each month, where natural gas is the main energy source.

For the solution chosen, the absorption refrigeration cycle requires 111.22 kg/s of hot water with an inlet temperature of 80°C to run the generator. To consider different alternatives to implement the absorption refrigeration cycle accounting for the efficient use of the solar energy, the four proposed scenarios are solved as follows:

Case A. Tanks storing at period $\theta = \theta'$ and dispatching at periods $\theta \neq \theta'$

Table 11 shows the maximum accumulation, volume and cost for each tank considered in the solution of the Case A. Notice that Tank 3 is too small compared with the rest of tanks (2.05 m^3). Tanks 1, 2 and 12 are not involved in the optimal solution to store hot water coming from the solar collector. It is noteworthy that the cold water tank has a volume of 426.70 m^3 and its cost is almost equivalent to the sum of the costs of the hot water storage tanks. The *TAC* for the storage tank system for this configuration is $512,958.47/year.

Table 9. Results Comparison for Example 1

Concept	Case A	Case C	Case D
Number of required tanks	11	11	9
Storage tanks system cost [$/year]	537,449.11	472,918.18	373,948.38
Cold water tank cost [$/year]	364,348.38	364,348.38	364,348.38
TAC [$/year]	901,797.49	837,266.56	738,296.76

Table 10. Stream Data for Example 2

Stream	Inlet temperature [°C]	Outlet temperature [°C]	*FCp* [kW/°C]
H1	65	60	1,060
H2	60	15	6.67
H3	57	15	33.33
H4	37	35	1,350
H5	120	35	50.59
H6	150	35	100.74
C1	95	97	2,900
C2	60	120	13.33
C3	95	110	193.33
C4	150	157	671.43

Case B. Tanks storing at periods $\theta \neq \theta'$ and dispatching at period $\theta = \theta'$

This operation mode has been modified to consider 24 tanks (a tank per hour, considering all the day) and not only the 12 h of solar radiation. Table 12 contains the solution obtained for this case, which has 10 hot tanks in addition to the cold water tank; in this figure, below each tank is shown the hour θ' when the tank dispatches hot water (most of them in periods when there is not available solar radiation). In this sense, each tank can receive hot water from the solar collector in the rest of the periods (periods available for storing considered by this operation mode); however, the storing is only possible during sunlight periods. Notice that only two tanks dispatch hot water when useful solar radiation is available (Tanks 2 and 9), whereas the other tanks dispatch during the part of the day without sunlight. In this sense, Tank 24 dispatches the working fluid from 5:00 am to 6:00 am and the storing is available since the dispatching has finished (6:00 am) until the next dispatching process starts (5:00 am) and the cycle is completed. Notice that the cold water tank has a volume significantly smaller than the size of the cold water tank obtained in Case A (341.85 m^3 vs. 426.70 m^3). Finally, the implementation of this scheme represents a *TAC* of $456,972.23/year.

Case C. Combination

In this configuration, 12 tanks can operate as Case A and other set of tanks operates as Case B only during the

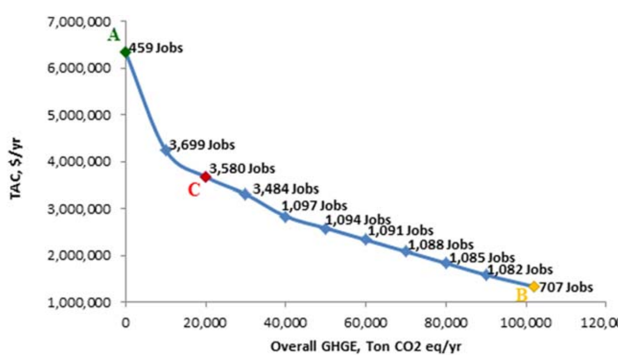

Figure 12. Pareto curve for Example 2.

[Color figure can be viewed in the online issue, which is available at wileyonlinelibrary.com.]

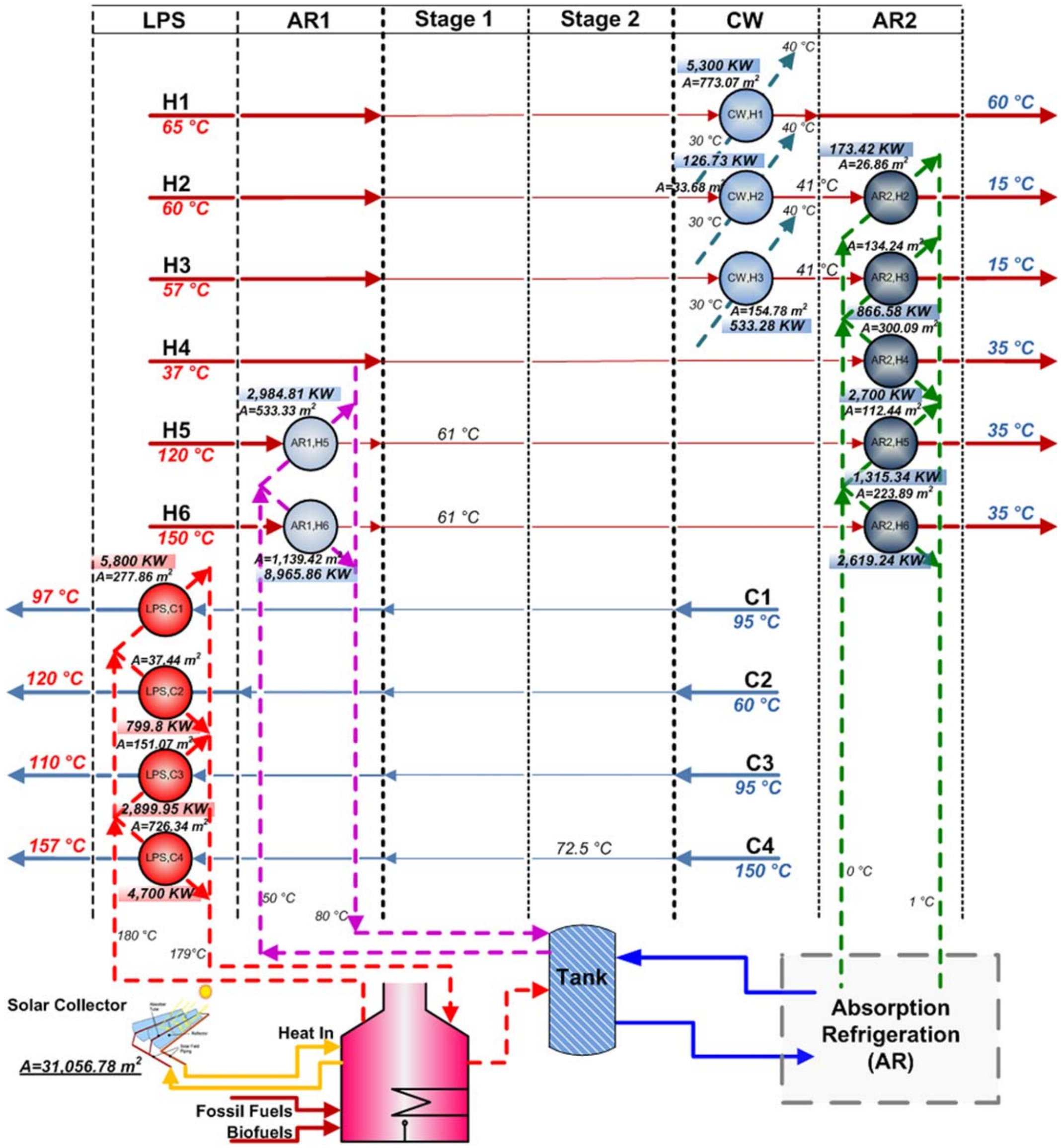

Figure 13. Integrated HEN and AR system obtained for Example 2.

[Color figure can be viewed in the online issue, which is available at wileyonlinelibrary.com.]

sunlight hours; nevertheless, the optimal solution only selects nine tanks operating as Case A (see Table 13). Although this solution is similar to the solution presented in Case A (the number of required tanks is the same in both cases), this case has a higher total annual cost (TAC of $561,145.63/year). Notice that this difference in cost between both solutions is due to the Tank 10 is bigger in Case C than in Case A (72.71 m^3 vs. 165.38 m^3).

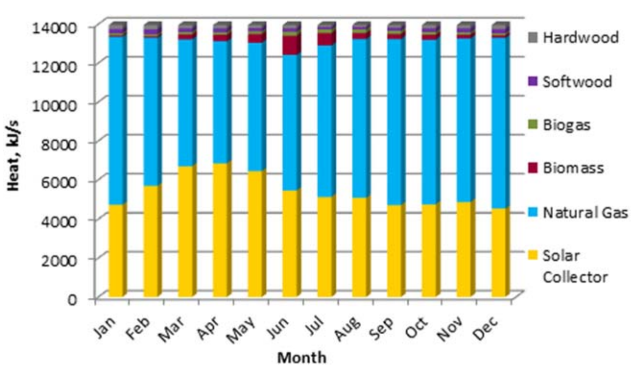

Figure 14. Energy sources required for each month for solution C of Example 2.

[Color figure can be viewed in the online issue, which is available at wileyonlinelibrary.com.]

Table 11. Solution for Case A of Example 2

Tank	Maximum Accumulation [kg/s]	Volume [m^3]	Cost [$]
3	0.57	2.05	2,264.34
4	14.05	50.59	27,507.63
5	16.73	60.24	32,525.40
6	22.10	79.54	42,560.96
7	20.32	73.16	39,241.51
8	21.19	76.27	40,862.64
9	19.13	68.85	37,002.81
10	20.20	72.71	39,009.92
11	14.80	53.26	28,897.16
Cold water tank	118.53	426.70	223,086.10

Table 12. Solution for Case B of Example 2

Tank	Maximum Accumulation [kg/s]	Volume [m^3]	Cost [$]
2	25.78	92.79	49,451.57
9	23.57	84.85	45,323.63
14	9.14	32.87	18,300.67
15	7.51	27.02	15,249.24
17	7.07	25.46	14,441.29
18	9.38	33.77	18,762.14
19	7.7	27.73	15,619.35
21	30.69	110.5	58,658.52
23	5.4	19.42	11,299.04
24	15.87	57.12	30,904.28
Cold water tank	94.96	341.85	178,962.50

Table 13. Solution for Case C of Example 2

Tank	Maximum Accumulation [kg/s]	Volume [m^3]	Cost [$]
Tanks operating as Case A			
3	0.57	2.05	2,264.34
4	14.05	50.59	27,507.63
5	16.73	60.24	32,525.40
6	22.10	79.54	42,560.96
7	20.32	73.16	39,241.51
8	21.19	76.27	40,862.64
9	19.13	68.85	37,002.81
10	45.94	165.38	87,197.00
11	14.80	53.26	28,897.16
Cold water tank	118.53	426.70	223,086.10

Table 14. Solution for Case D of Example 2

Tank	Maximum Accumulation [kg/s]	Volume [m^3]	Cost [$]
1	7.14	25.72	14,574.22
2	10.64	38.31	21,118.64
3	4.99	17.98	10,547.65
4	17.79	64.04	34,502.12
5	21.80	78.46	42,000.76
6	11.85	42.67	23,386.81
7	25.63	92.29	49,190.18
8	4.89	17.60	10,353.49
9	8.20	29.52	16,548.54
10	5.59	20.12	11,663.71
Cold water tank	118.53	426.70	223,086.10

Case D. Disjunctive model

This case includes an important number of binary variables to allow inlet flow rates and outlet flow rates in each tank at any time but not at the same time. Table 14 presents the optimal solution for this operation mode, which has 10 hot tanks. The cold water tank has a volume of 426.70 m^3. Additionally, the tank sizes found in this solution are significantly lower than those of previous solutions for this example and, as consequence, the tank costs are smaller respect to the other solutions; in this case, the total annual cost is $456,972.22/year.

Moreover, the costs comparison of the four cases considered in the case study is shown in Table 15. Case C represents the worst economic solution with a TAC of $561,145.63/year, while Cases B and D are the best solutions found with a TAC of $456,972.23/year, which represents a reduction of 18.56% respect to Case C. Then, Cases B and D have the same total annual cost and both required 10 tanks in the optimal solution; however, notice that the solution for Case B is different than the one for Case D, owing to the cold water tank size in Case D is larger, but in Case B the hot storage tanks system cost is higher. An intermediate solution is represented by the solution of Case A, which requires nine tanks and a total annual cost of $512,958.47/year.

It is noteworthy that the internal flow rates, temperatures and accumulations of the proposed configuration are determined for each case considering their variation during the day and months.

Finally, Table 16 shows the problem characteristics for both stages of the two examples illustrated. In this sense, the second stage contains the same characteristics for Example 1 and Example 2 and only varies for the different scenarios analyzed. Notice that for scenario D the problem size is significantly greater and so the CPU required in a computer with an i7 processor at 3.4 GHz and 16 GB of RAM.

Conclusion

This article has presented a two-step approach for the optimal design of HENs integrated with absorption refrigeration cycles involving the utility selection from a set of available energy sources that include fossil fuels, biofuels and solar collectors. A multitank sensible energy storage system that uses liquid water as both the heat transfer fluid and the storage media has been proposed. The variation in the hourly radiation of solar energy is taken into account. Furthermore, the seasonal variability of biofuels and fossil fuels was

Table 15. Results comparison for Example 2

Concept	Case A	Case B	Case C	Case D
Number of tanks required	9	10	9	10
Storage tanks system cost [$/year]	289,872.37	278,009.73	338,059.53	233,886.12
Cold water tank cost [$/year]	223,086.10	178,962.50	223,086.10	223,086.10
TAC [$/year]	512,958.47	456,972.23	561,145.63	456,972.22

Table 16. Characteristics for the Proposed Methodology in the Examples

	Stage 1		Stage 2			
Concept	Example 1	Example 2	Case A	Case B	Case C	Case D
Number of constraints	355	481	13,875	24,567	24,567	17,563
Number of continuous variables	318	452	17,645	31,541	31,541	18,206
Number of binary variables	43	78	0	0	0	2,880
CPU time (sec)	0.062	0.047	0.093	0.467	0.484	0.266

considered in the proposed formulation that is based on mixed integer nonlinear programming methods. The first step of this methodology optimizes the configuration and design of the HEN coupled to the AR cycle without heat storage on a monthly basis. The first optimization step provides the optimal energy integration of the HEN with the AR cycle considering simultaneously the minimization of the total annual cost, the minimization of the overall greenhouse gas emissions and accounting for the number of jobs that can be created for the use of the different types of energy sources. In this step the HEN configuration, use of external energies (solar, biofuels and fossil fuels) as well as the type and size of the solar collector needed are determined. In the second step the optimal design and operation of the multi-tank TES system (number of storage tanks and their optimal size) are determined. The proposed formulation considers different tank operation modes to find the best tradeoff between TAC and operation. Two case studies have been solved to show the applicability of the proposed methodology. The results show that the proposed approach is capable of producing designs and operating schedules that integrate various forms of energy while accounting for economic, environmental and social metrics.

Notation

Parameters

$Avail$ = maximum availability, kg/month
C = cost, \$
COP = coefficient of performance
Cp^{Fluid} = specific heat capacity of the fluid, kJ/kg K
Cu = unit operating cost, \$/kJ
D_m^{dm} = conversion factor, day/month
D^{sh} = conversion factor, s/h
D_t = conversion factor, s/month
F^{Pro} = flow rate required by the AR cycle, kg/s
FC = fixed charge, \$/y
FCp = heat capacity flow rate, kJ/s K
$GHGE$ = greenhouse gas emissions, ton CO_{2eq}/kJ
H = film heat transfer coefficient, kW/m^2 K
HPS = $i \mid i$ is a hot process stream
$Heating^{Power}$ = heating power, kJ/kg
H_Y = hours of operation per year, h/y
k_f = factor used to annualize the capital costs
$NJOBS$ = unit number of generated jobs, jobs
NOK = total number of stages
Q^{Useful} = usable solar radiation in the specific location, kJ/m^2 month
R = tax credit for the reduction of $GHGE$, \$/kJ
T^{IN} = inlet temperature, K
T^{OUT} = outlet temperature, K
$T^{Process\_In}$ = inlet temperature to the AR system, K
$T^{Process\_Out}$ = outlet temperature to the AR system, K
$T^{Vaporization}$ = vaporization temperature of the working fluid, K
VC = variable charge, \$m^3 yr

Greek letters

α = combustion efficiency
β = exponent for tank cost and for area cost
δ = small number
θ = index for hours of the day (24 slots)
ρ = density
τ = residence time
$\Delta T^{\max}$ = upper bound for temperature difference, K
$\Delta T_{\min}$ = minimum approach temperature difference, K
Θ = set for hours

Variables

a_c = area of the solar collector, m^2
$cost^{Tank}$ = of the tank p, \$/yr
$cost^{WT}$ = water tank cost, \$/yr
dt = temperature approach difference, K
f^{By} = bypass flow rate to avoid the solar collector, kg/s
f^{coll} = flow rate leaving the solar collector, kg/s
f^{Mix} = output stream from the storage tank system, kg/s
f^{TankBy} = bypass flow rate to avoid the storage tanks, kg/s
f^{Tank_In} = flow rate entering to the storage tank p, kg/s
f^{Tank_Out} = flow rate leaving form the storage tank p, kg/s
f^{WT_Out} = flow rate leaving the water tank, kg/s
q = heat exchanged, kJ/s
$q^{External}$ = external heat required by the AR system, kJ/s
q^{Heater} = heat transferred in the heater, kJ/s
q^{Loss} = heat losses in the tank p, kJ/s
q^{Solar} = total solar energy, kJ/month
sa = mass accumulation, kg/s
sa_0 = initial mass accumulation, kg/s
$t_{i,k}$ = internal temperature, K
tac = total annual cost, \$/y
t^{Heater} = temperature entering to the heater, K
t^{Mix} = temperature of the output stream from the storage tank system, K
t^{Solar} = temperature at the exit of the solar collector, K
t^{Tank} = temperature in the tank p, K
$t^{Tank\_Initial}$ = initial temperature in the tank p, K
v_p^{Tank} = volume of the storage tank p, K
v^{WT} = water tank volume, m^3
W = Boolean variables used to model the existence of the type of solar collector
w = binary variables to model the existence of the type of solar collector
Y = Boolean variables used to model the existence of a solar collector
y = binary variables to model the existence of a solar collector
Y_p = Boolean variables used to model the existence of the storage tanks
y_p = binary variable to model the existence of the storage tank p
Z = Boolean variables used to model the possible existence of inlet or outlet flow rates in the storage tanks
z = binary variables to model the possible existence of inlet or outlet flow rates in the storage tanks

Sets

B = $b \mid b$ is a biofuel
CPS = $j \mid j$ is a cold process stream
F = $f \mid f$ is a fossil fuel
G = $g \mid g$ is a segment for the capital cost of the solar collector
HPS = $i \mid i$ is a hot process stream
M = $m \mid m$ is a month
P = $p \mid p$ is a storage tank
S = $s \mid s$ is a solar collector
ST = $k \mid k$ is a stage in the superstructure, $k = 1, \ldots,$ NOK
Θ = $\theta \mid \theta$ is an hour

Subscripts and superscripts

$ar1$ = stage of the superstructure where the excess heat from hot process streams is removed
$ar2$ = stage of the superstructure where the hot process streams are cooled
b = biofuels
cap = capital
cw = cold water
dis = disaggregated
f = fossil fuel
i = hot process stream
j = cold process stream
k = index for stage (1, …, NOK) and temperature location (1, …, NOK + 1)
LPS = stage of the superstructure where the cold process streams exchange heat with low-pressure steam
m = month
Max = maximum
Out = outlet
op = operational
p = tank
r = segment for the capital cost for the solar collectors
s = solar collector
t = period of time (i.e., months)

Tank = storage tank
Up = maximum allowable
WT = water tank placed at the exit of the AR system
θ = p (i.e., hours)

Acknowledgment

This research was supported by the Mexican Council for Science and Technology (CONACYT), and the Council for Scientific Research of the UMSNH, which is gratefully acknowledged by the authors.

Literature Cited

1. Kim JK. Smith R. Cooling water system design. *Chem Eng Sci*. 2010;56(12):3641–58.
2. Picón-Núñez M, Polley GT, Canizalez-Dávalos L, Medina-Flores JM. Short cut performance method for the design of flexible cooling systems. *Energy*. 2011;36(8):4646–53.
3. Cortinovis GF, Ribeiro MT, Paiva JL, Song TW, Pinto JM. Integrated analysis of cooling water systems: modeling and experimental validation. *Appl Therm Eng*. 2009;29(14-15):3124–31.
4. Ponce-Ortega JM, Serna-Gonzalez M, Jimenez-Gutierrez A. Optimization model for re-circulating cooling water systems. *Comput Chem Eng*. 2010;34(2):177–95.
5. Ponce-Ortega JM, Serna-Gonzalez M, Jimenez-Gutierrez A. A disjunctive programming model for simultaneous synthesis and detailed design of cooling networks. *Ind Eng Chem Res*. 2009;48(6):2991–3003.
6. Ponce-Ortega JM, Serna-Gonzalez M, Jimenez-Gutierrez A. MINLP synthesis of optimal cooling networks. *Chem Eng Sci*. 2007;62(21): 5728–35.
7. Rubio-Castro E, Serna-Gonzalez M, Ponce-Ortega JM, El-Halwagi MM. Synthesis of cooling water systems with multiple cooling towers. *Appl Therm Eng*. 2013;50(1):957–74.
8. Rubio-Castro E, Serna-Gonzalez M, Ponce-Ortega JM. Optimal design of effluent-cooling systems using a mathematical programming model. *Appl Therm Eng*. 2010;30(14-15):2116–2126.
9. Smith R. Chemical Process Design and Integration. Hoboken, NJ: John Wiley & Sons, Ltd; 2005.
10. El-Halwagi MM. Sustainable design through process integration. *Butterworth-Heinemann* 2011.
11. Ziegler F, Riesch P. Absorption cycles, a review with regard to energetic efficiency. *Heat Recovery Systems CHP*. 1993;13(2):147–59.
12. Herold K, Radermacher R, Kleint SA. Absorption Chillers and Heat Pumps. Boca Raton, FL: CRC Press; 1996.
13. Chavéz-Islas LM, Heard CL. Design and analysis of an ammonia/water absorption refrigeration cycle by means of an equation-oriented method. *Ind Eng Chem Res*. 2009;48(4):1944–56.
14. Chavéz-Islas LM, Heard CL. Optimization of a simple ammonia-water absorption refrigeration cycle by application of mixed-integer nonlinear programming. *Ind Eng Chem Res*. 2009;48(4):1957–72.
15. Chavéz-Islas LM, Heard CL, Grossmann IE. Synthesis and optimization of an ammonia-water absorption refrigeration cycle considering different types of heat exchangers by application of mixed-integer nonlinear programming. *Ind Eng Chem Res*. 2009;48(6):2972–2990.
16. Florides GA, Kalogirou SA, Tassou SA, Wrobel LC. Modelling, simulation and warming impact assessment of a domestic-size absorption solar cooling system. *Appl Therm Eng*. 2002;22(12):1313–25.
17. Florides GA, Kalogirou SA, Tassou SA, Wrobel LC. Modelling and simulation of an absorption solar cooling system for cyprus. *Solar Energy*. 2002;72(1):43–51.
18. Assilzadeh F, Kalogirou SA, Ali Y, Sopian K. Simulation and optimization of a LiBr solar absorption cooling system with evacuated tube collectors. *Renew Energy*. 2005;30(8):1143–59.
19. Lecuona A, Ventas R, Venegas M, Zacarías A, Salgado R. Optimum hot water temperature for absorption solar cooling. *Solar Energy*. 2009;83(10):1806–14.
20. Fathi R, Guemimi C, Ouaskit S. An irreversible thermodynamic model for solar absorption refrigerator. *Renew Energy*. 2004;29(8):1349–65.
21. Wu C, Chen L, Sun F. Optimization of solar absorption refrigerator. *Appl Therm Eng*. 1997;17(2):203–8.
22. Savola T, Fogelholm CJ. MINLP optimization model for increased power production in small-scale CHP plants. *Appl Therm Eng*. 2007; 27(1):89–99.
23. Tveit TM, Savola T, Gebremedhin A, Fogelholm CJ. Multi-period MINLP model for optimizing operation and structural changes to CHP plants in district heating networks with long-term thermal storage. *Energy Conversion Manage*. 2009;50(3):639–647.
24. Hamed M, Fellah A, Brahim AB. Optimization of a solar driven absorption refrigerator. *Appl Energy*. 2012;92(6):714–724.
25. Gebreslassie BH, Guillén-Gosálvez G, Jiménez L, Boer D. Design of environmentally conscious absorption cooling systems via multi-objective optimization and life cycle assessment. *Appl Energy*. 2009; 86(9):1712–22.
26. Gebreslassie BH, Guillén-Gosálvez G, Jiménez L, Boer D. Economic performance optimization of an absorption cooling system under uncertainty. *Appl Therm Eng*. 2009;29(17-18):3491–3500.
27. Gebreslassie BH, Guillén-Gosálvez G, Jiménez L, Boer D. A systematic tool for the minimization of the life cycle impact of solar assisted absorption cooling systems. *Appl Energy*. 2009;35(9):3849–62.
28. Ponce-Ortega JM, Tora EA, González-Campos JB, El-Halwagi MM. Integration of renewable energy with industrial absorption refrigeration systems: systematic design and operation with technical, economic and environmental objectives. *Ind Eng Chem Res*. 2011; 50(16):9667–84.
29. Lira-Barragán LF, Ponce-Ortega JM, Serna-Gonzalez M. El-Halwagi, MM. Synthesis of integrated absorption refrigeration systems involving economic and environmental objectives and quantifying social benefits. *Appl Therm Eng*. 2013;52(2):402–419.
30. Gundersen T, Naess L. The synthesis of cost optimal heat exchanger network-an industrial review of the state-of-the art. *Comput Chem Eng*. 1988;12(6):503–530.
31. Jezowski J. Heat exchanger network grassroot and retrofit design-The review of the state-of the-Art. 1. Heat-exchanger network targeting and insight based methods of synthesis. *Hung J Ind Chem*. 1994; 22(4):279–94.
32. Jezowski J. Heat-exchanger network grassroot and retrofit design-The review of the state-of-the-art. 2. Heat-exchanger network synthesis by mathematical-methods and approaches for retrofit design. *Hung J Ind Chem*. 1994;22(4):295–308.
33. Furman KC, Sahinidis NV. A critical review and annotated bibliography for heat exchanger network synthesis in the 20th century. *Ind Eng Chem Res*. 2002;41(10):2335–70.
34. Morar M, Agachi PS. Review: Important contributions in development and improvement of the heat integration techniques. *Comput Chem Eng*. 2010;34(8):1171–9.
35. Linnhoff B, Hindmarsh E. The pinch design method for heat exchanger networks. *Chemical Engineering Science*. 1983;38(5): 745–63.
36. Linnhoff B, Ahmad S. Cost optimum heat exchanger networks 1. Minimum energy and capital using simple-models for capital costs. *Comput Chem Eng*. 1990;14(7):729–50.
37. Shenoy UV. Heat Exchanger Network Synthesis: Process Optimization by Energy and Resource Analysis. Houston, TX: Gulf Publishing Co.; 1995.
38. Castier M. Rigorous multiple utility targeting in heat exchanger networks. *Energy Convers Manage*. 2012;59(2):74–85.
39. Yee TF, Grossmann IE. Simultaneous optimization models for heat integration-II. Heat exchanger network synthesis. *Comput Chem Eng*. 1990;14(10):1165–84.
40. Lopez-Maldonado LA, Ponce-Ortega JM, Segovia-Hernandez JG. Mutiobjective synthesis of heat exchanger networks minimizing the total annual cost and the environmental impact. *Appl Therm Eng*. 2011;31(6-7):1099–1113.
41. Ponce-Ortega JM, Serna-Gonzalez M, Jimenez-Gutierrez A. Synthesis of heat exchanger networks with optimal placement of multiple utilities. *Ind Eng Chem Res*. 2010;49(6):2849–56.
42. Lewin DR. A generalized method for HEN synthesis using stochastic optimization-II The synthesis of cost-optimal networks. *Comput Chem Eng*. 1998;22(10):1387–1405.
43. Lewin DR, Wang O. Shalev, A generalized method for HEN synthesis using stochastic optimization e I. General framework and MER optimal synthesis. *Comput Chem Eng*. 1998;22(10):1503–13.
44. Yu H, Fang H, Yao P, Yi Y. A combined genetic algorithm/simulated annealing algorithm for large scale system energy integration. *Comput Chem Eng*. 2000;24(8):2023–2035.
45. Ravagnani MASS, Silva AP, Arroyo PA, Constantino AA. Heat exchanger network synthesis and optimization using genetic algorithm. *Appl Therm Eng*. 2005;25(7):1003–17.
46. Allen B, Sarvard-Goguen M, Gosselin L. Optimization of heat exchanger networks with genetic algorithms for designing each heat exchanger including condensers. *Appl Therm Eng*. 2009;29(16):3437–3444.

47. Lin B, Miller DC. Solving heat exchanger network synthesis problem with tabu search. *Comput Chem Eng*. 2004;28(8):1451–64.
48. Silva AP, Ravagnani MASS, Biscaia EC, Caballero JA. Optimal heat exchanger network synthesis using particle swarm optimization. *Optimiz Eng*. 2010;11(3):459–70.
49. Athier G, Floquet P, Pibouleau L, Domenech S. Synthesis of heat exchanger networks by simulated annealing and NLP procedures. *AIChE J*. 1997;43(11):3007–19.
50. Dolan WB, Cummings PT, Van MDL. Process optimization via simulated annealing: application to network design. *AIChE J*. 1989; 35(5):725–36.
51. Lotfi R, Boozarjomehry RB. Superstructure optimization in heat exchanger network (HEN) synthesis using modular simulators and a genetic algorithm. *Ind Eng Chem Res*. 2010;49(10):4731–7.
52. Ponce-Ortega JM, Serna-Gonzalez M, Jimenez-Gutierrez A. Synthesis of multipass heat exchanger networks using genetic algorithms. *Comput Chem Eng*. 2008;320(10):2320–32.
53. Çetinkaya E, Rosen MA, Dinçer I. Life cycle assessment of a fluidized bed system for steam production. *Energy Conver Manage*. 2012;63:225–32.
54. Burnham A, Wang M, Wu Yi. Development and application of GREET 2.7 - the transportation cycle model, ANL/ESD/06-5 and GREET 2.7. http://www.transportation.anl.gov/modeling_simulation/GREET/index.htm. Accessed April 14, 2013.
55. Goldberg M, Sinclair K, Milligan M. Job and economic development impact (JEDI) model: a user-friendly tool to calculate economic impacts from wind projects. 2004 Global Windpower Conference. 2004;NREL/CP-500–35953.
56. Mendez CA, Cerda J, Grossmann IE, Harjunkoski I, Fahl M. State-of-the-art review of optimization methods for short-term scheduling of batch processes. *Comput Chem Eng*. 2006;30(6−7):913–46.
57. Floudas CA, Lin X. Continuous-time versus discrete-time approaches for scheduling of chemical processes: A review. *Comput Chem Eng*. 2004;28(11):2109–29.
58. Kallrath J. Planning and Scheduling in the Process Industry. *OR Spectrum*. 2002;24(3):219–50.
59. Barbosa-Povoa A. A critical review on the design and retrofit of batch plants. *Comput Chem Eng*. 2007;31(7):833–855.
60. Mouret S, Grossmann IE, Pestiaux P. A new lagrangian decomposition approach applied to the integration of refinery planning and crude-oil scheduling. *Comput Chem Eng*. 2011;35(12):2750–66.
61. Mouret S, Grossmann IE, Pestiaux P. A Novel priority-slot based continuous-time formulation for crude-oil scheduling problems. *Ind Eng Chem Res*. 2009;48(18):8515–28.
62. Sharda B, Vazquez A. Evaluating capacity and expansion opportunities at tank farm: A decision support system using discrete event simulation. Proceedings of the 2009 Winter Simulation Conference; Institute of Electrical and Electronic Engineers: New York; 2009; 2218−2224.
63. Terrazas-Moreno S, Grossmann IE, Wassick JM. A mixed-integer linear programming model for optimization the scheduling and assignment of tank farm operation. *Ind Eng Chem Res*. 2012;51(18): 6441–54.
64. Gutiérrez-Limón MA, Flores-Tlacuahuac A, Grossmann IE. A multiobjetive optimization approach for simultaneous single line scheduling and control of CSTRs. *Ind Eng Chem Res*. 2012;51(17): 5881–90.
65. Erdirik-Dogan M, Grossmann IE. Simultaneous planning and scheduling of single-stage multiproduct continuous plants with parallel lines. *Comput Chem Eng*. 2008;32(11):2664−83.
66. Barbosa-Povoa A, Macchietto S. Detailed design of multipurpose batch plants. *Comput Chem Eng*. 1994;18(11-12):1013–1042.
67. Lin X, Floudas C. Design, synthesis and scheduling of multipurpose batch plants via an effective continuous-time formulation. *Comput Chem Eng*. 2001;25(4-6):665.
68. Castro P, Barbosa-Povoa A, Novais A. Simultaneous design and scheduling of multipurpose plants using resource task network based continuous-time formulations. *Ind Eng Chem Res*. 2005;44(2):343–357.
69. Tora EA, El-Halwagi MM. Optimal design and integration of solar systems and fossil fuels for sustainable and stable power outlet. *Clean Technologies Environ Policy*. 2009;11(4):401–7.
70. Diwekar UM. Introduction to applied optimization and modeling. Kluwer Academic Publishers: Dordrecht, The Netherlands: Houston, TX; 2003.
71. Chen JJJ. Letter to the editor: Comments on improvement on a replacement for the logarithmic mean. *Chem Eng Sci*. 1987;42(10): 2488–2489.
72. Sözen A. Effect of heat exchangers on performance of absorption refrigeration systems. *Energy Convers Manage*. 2001;42(14):1699–716.
73. Joudi KA, Lafta AH. Simulation of a simple absorption refrigeration system. *Energy Convers Manage*. 2001;42(13):1575–1605.
74. Dincer I, Edin M, Ture IE. Investigation of thermal performance of a solar powered refrigeration system. *Energy Convers Manage*. 1996;37(1):51–58.
75. Kumar R, Kaushik SC. Thermodynamic evaluation of a modified aqua-ammonia absorption refrigeration system. *Energy Convers Manage*. 1991;32(2):191–95.
76. .http://eosweb.larc.nasa.gov/sse/RETScreen/.
77. Coskun C, Oktay Z, Dincer I. Estimation of monthly solar radiation distribution for solar energy system analysis. *Energy*. 2011;36(2): 1319–23.
78. Fernández-García A, Zarza E, Valenzuela L, Pérez M. Parabolic-trough solar collectors and their applications. *Renew Sustain Energy Rev*. 2010;14(7):1695–721.
79. Solanki CS, Sangani CS. Estimation of monthly averaged direct normal solar radiation using elevation angle for any location. *Solar Energy Mater Solar Cells*. 2008;92(1):38–44.
80. Srivastava SK, Singh OP, Pandey GN. Correlations for the estimation of hourly global solar radiation. *Appl Energy*. 1995;52(1):55–64.
81. Brooke A, Kendrick D, Meeruas A, Raman R. *GAMS-Language Guide*. Washington, DC: GAMS Development Corp.; 2012.
82. Rubio-Castro E, Ponce-Ortega JM, Serna-González M, El-Halwagi MM, Pham V. Global optimization in property-based inter-plant water integration. *AIChE J*. 2013;59(3):813–833.

Manuscript received May 2, 2013, and revision received Nov. 6, 2013.